CrystEngComm

HIGHLIGHT

View Article Online
View Journal | View Issue

Cite this: *CrystEngComm*, 2016, **18**, 4218

Smart, stretchable and wearable supercapacitors: prospects and challenges

Yu Zheng, Yanbing Yang, Shasha Chen and Quan Yuan*

Received 21st December 2015, Accepted 5th February 2016

DOI: 10.1039/c5ce02510a

www.rsc.org/crystengcomm

Among the various energy storage systems, supercapacitors are considered to be the most promising alternative to batteries due to their high power density, long cycle life and fast charge–discharge process. Especially, flexible electrochemical supercapacitors with their unique advantages such as flexibility, shape-conformability, and light weight are attracting ever-increasing attention to meet the current requirements for portable and wearable electric devices in modern energy storage markets. In this perspective, we summarize the most recent progress in flexible all-solid supercapacitors from the point of view of flexible electrode materials. Various flexible electrode materials like carbon nanotubes, graphene, and pseudo capacitive materials are discussed and their performance is comprehensively analyzed. In addition, an overview of the latest progress in strategies to improve the energy and power density is discussed. Further research targets in multifunctional integrated systems and challenges in realizing idealized flexible energy storage systems are also proposed.

1. Introduction

Serious climate change and decreasing availability of fossil fuels have compelled people to search for renewable energy production techniques and resources.[1,2] As a result, one solution to solve this problem is the development of efficient electrochemical energy storage systems with high energy and power characteristics to fulfill the requirements for inexpensive, flexible, light-weight and environmentally friendly energy storage devices.[3–21] Supercapacitors (SCs), also known as electrochemical capacitors or ultracapacitors, are considered to hold the most promise for mobile energy storage technology because of their advantages such as ultrafast power supply, high energy density and long cycle life.[22–25] Fig. 1 illustrates the 'Ragone plot' of specific power *versus* specific energy for various energy storage devices.[24] In comparison with other energy storage devices, SCs exhibit the highest specific power and appropriate energy density, making them powerful alternative candidates for batteries in the energy storage field.

More recently, accompanied with the development of portable and wearable electronic devices for specific applications such as bendable smart phones, flexible wireless sensors and

College of Chemistry and Molecular Sciences, Wuhan University, Wuhan 430072, China. E-mail: yuanquan@whu.edu.cn

Yu Zheng

Yu Zheng is presently an undergraduate student at the College of Chemistry and Molecular Sciences, Wuhan University. She is currently working in Prof. Quan Yuan's group. Her research interest is focused on the development of flexible all-solid supercapacitors as energy storage devices.

Yanbing Yang

Yanbing Yang is currently a PhD candidate at the College of Chemistry and Molecular Sciences, Wuhan University. Her research interests are mainly focused on the controlled growth of carbon nanotube sponges, synthesis of hierarchical porous materials and exploring their applications in energy storage systems, such as supercapacitors and lithium batteries.

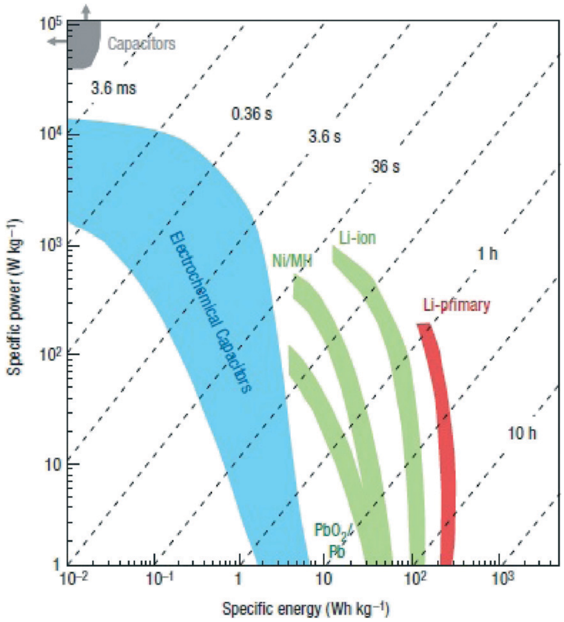

Fig. 1 Ragone plot of specific power *versus* specific energy for various energy storage devices. Reproduced with permission from ref. 24. Copyright 2008, Nature Publishing Group.

wearable biomedical devices, great interests has been aroused in flexible energy storage equipment.[26–36] Flexible all-solid state SCs, because of their outstanding advantages like ultra-flexibility, small size, light weight, and ease of operation,[37–41] hold great promise as a new kind of flexible energy storage systems for applications in hybrid electric vehicles, memory backup systems, and portable electronic devices.[42] In addition, the ability to withstand a wide range of high tensile strain conditions like bending, folding and even twisting makes SCs particularly suitable for wearable electronics, which can be operated at various situations without performance degradation.[43] Up to now, considerable attempts have been made to fabricate flexible SCs with multiple geometries including planar, fiber and wire-shape to obtain multi-functional integrated systems and micro-scale devices.[44–49]

In general, the performance of a supercapacitor mainly depends on several key components including the electrode, electrolyte, and device configuration.[24,50,51] Current research on flexible SCs has achieved great advances from the aspect of electrode materials including carbon nanotubes, graphene, transition metal oxides, conductive polymers and their combined composites. Here, we give a brief summary of the recent progress in flexible SCs. First we review the electrode materials of flexible SCs, and further a comprehensive study of the performance and storage mechanism is discussed. An analysis of the strategies to improve the electrochemical storage performance of flexible SCs is given. Finally, we introduce the future challenges and opportunities that flexible SCs might face. The latest development of multifunctional systems which combine energy conversion and storage into one unit is discussed.

2. Flexible devices

Flexible SCs is an emerging field in the area of energy storage wherein circuits can be built on flexible substrates. The designed configuration has the capacity to accommodate large levels of strain while maintaining superior electronic

Shasha Chen

Shasha Chen is currently a graduate student at the College of Chemistry and Molecular Sciences, Wuhan University. Her research interest is mainly focused on developing flexible lithium ion batteries and supercapacitors based on carbon nanotubes.

Quan Yuan

Quan Yuan is currently a full professor in the College of Chemistry and Molecular Sciences at Wuhan University. She received her BS degree (2004) from Wuhan University, China, and her PhD (2009) in Inorganic Chemistry from Peking University, China. Later, she performed postdoctoral research (2009–2012) at the University of Florida. Her research interests involve the controlled synthesis of functional nanomaterials and investigating their corresponding biomedical applications. Up till now, Prof. Yuan has won many awards such as the National Top 100 Doctoral Thesis (2011) and Excellent Young Scientist Foundation of NSFC (2014). Currently, she has published 46 high-quality papers on journals like Proc. Natl. Acad. Sci., J. Am. Chem. Soc., Angew. Chem., Int. Ed., etc.

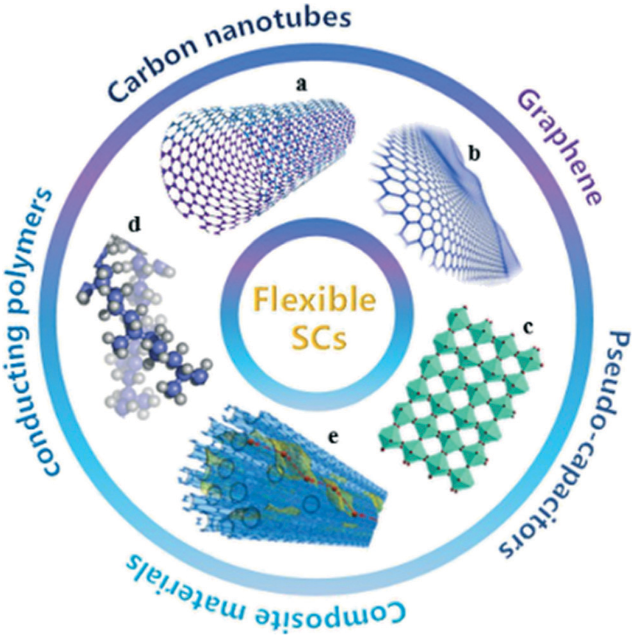

Fig. 2 Structure models of typical flexible electrode materials: (a) carbon nanotubes (CNTs), (b) graphene, (c) pseudo-capacitors, (d) conducting polymers, (e) composite materials. (e) Reproduced with permission from ref. 189. Copyright 2014 WILEY-VCH Verlag GmbH & Co. KGaA, Weinheim.

performance.[43,71] In comparison with conventional SCs, flexible SCs hold great promise to act as storage units in portable devices and wearable electronics.[4,9,10,72–81] The excellent performance comes from their unique advantages, such as the ability to withstand a wide range of strain, shape diversity and light weight.[37–41] The key to fabricate flexible SCs lies in the electrode materials which have good electrical and mechanical properties.[52–71] Typically, the current reported flexible electrode materials (Fig. 2) include carbon nanotubes, graphene, transitional metal oxides, conductive polymers as well as their combined composites. Other than the flexible electrode materials, a soft substrate[82–84] is another important component needed to provide the shape variable support. The integration of flexible electrode materials into various flexible substrates, such as plastic, textile, sponge and paper, has been widely reported.[85–94]

3. Flexible electrode materials

3.1. Carbon nanotubes (CNTs)

CNTs, due to their good electrical conductivity (104–105 S cm^{-1}), high specific surface area (1240–2200 $m^2\ g^{-1}$), unique porous structure, and superior mechanical and thermal stability have attracted a great deal of attention as supercapacitor electrodes.[95–104] Moreover, their high aspect ratio and open tubular network make them excellent electrode materials for flexible SCs.[100,105] Niu *et al.*[13] fabricated highly integrated stretchable SCs based on buckled single-walled carbon nanotube (SWCNT) films. These buckled SWCNT film electrodes (Fig. 3a) were synthesized by combining directly

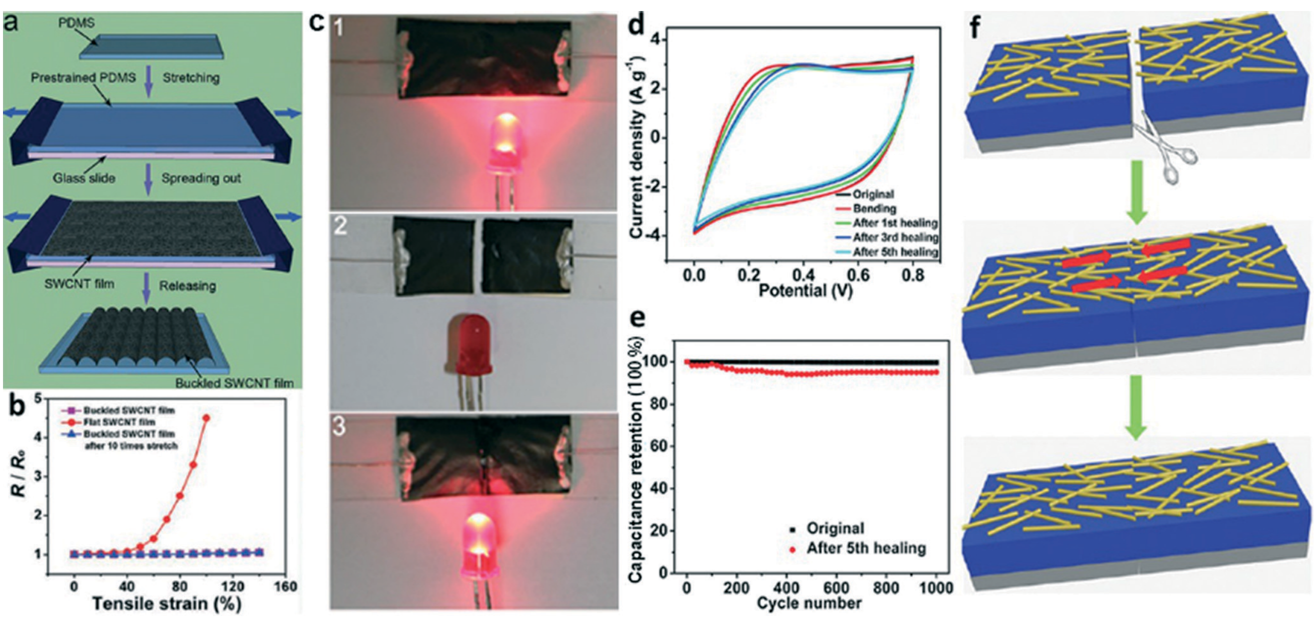

Fig. 3 (a) Schematic of preparing a buckled SWCNT film on PDMS. (b) The normalized sheet resistance of SWCNT films on PDMS with and without buckled structure at different strain levels and buckled SWCNT film after 10 times stretching at different strain levels, where R_0 is the resistance of the unstretched SWCNT films and R is the resistance of the SWCNT films at different strain levels. (a, b) Reproduce with permission from ref. 132. Copyright 2013 WILEY-VCH Verlag GmbH & Co. KGaA, Weinheim. (c) Optical images of as-prepared SWCNT films spread on self-healing substrates in a circuit with an LED bulb. (c1) the original; (c2) after cutting; (c3) after healing. (d) Cyclic voltammograms of the device under bending (an inward ~45° bending angle) and after healing for different times. (e) Capacitance retention of the devices before cutting and after the 5th healing after 1000 cycles under a current density of 5 A g^{-1}. (f) Schematic representation of self-healing capabilities of electrical conductivity of as-prepared SWCNT films spread on self-healing substrates. (c–f) Reproduced with permission from ref. 91. Copyright 2014 Wiley-VCH Verlag GmbH & Co. KGaA, Weinheim.

grown SWNT network films with a polydimethylsiloxane (PDMS) substrate with enhanced pre-strain. Given that the ability of enduring strain is a function of the wavelength of the buckled structure, a large pre-strain applied to the PDMS substrate will form a smaller wavelength of the buckled structure. Thus, by increasing the pre-strain of PDMS, they fabricated the buckled SWCNT film electrodes, whose periodic buckling wavelength is about 1.1 μm which is smaller than other reported buckled SWCNT film electrodes (2 μm). These electrodes can be stretched under a strain of 140% without a significant change of resistance (Fig. 3b). Using the H_2SO_4-PVA gel as both an electrolyte and separator, the capacitance retention of the prepared integrated highly stretchable SWNT film supercapacitor almost remains unchanged even under 120% strain during the charge/discharge process.

Despite the superior flexibility of integrated devices, the electrode materials become susceptible to structure fractures under bending or during charge and discharge processes when subjected to practical applications.[106–110] Thus, it should be of scientific and technological importance to explore robust supercapacitors with the capability of managing mechanical damage. Polymer flexible substrates may possibly undergo mechanical damage caused by deformation or incident cutting. Self-healing materials, which can repair the internal or external damage that they have experienced, promised their applications for developing functional devices with robust mechanical flexibility and excellent stability.[111–126] Wang *et al.*[91] reported a mechanical and electrical self-healing supercapacitor (Fig. 3c) by spreading SWNT films onto self-healing substrates. The self-healing composites are composed of supermolecular network supported hierarchical flower-like TiO_2 nanostructures, whose lateral movement can bring the fracture surfaces into contact with each other in the event of cutting or breakage (Fig. 3f). Moreover, the existence of a PVP-H_2SO_4 gel electrolyte with self-adhering performance enhances the self-healing efficiency. As a result, the as-prepared supercapacitors exhibit excellent electrochemical storage (Fig. 3d) and self-healing performance, and the specific capacitance (Fig. 3e) can be restored up to 85.7% of its original value even after the 5th cutting.

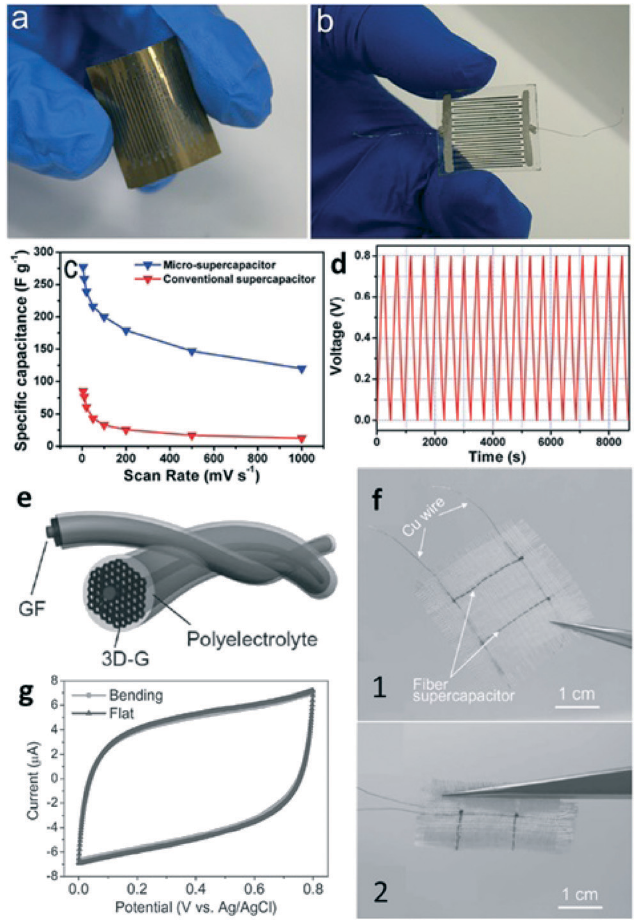

Fig. 4 (a) Optical images of rGO patterns on PET with Au film. (b) Optical images of micro-supercapacitors on PET. (c) The specific capacitance of the rGO micro-supercapacitor and conventional supercapacitor at different scan rates. (d) Typical galvanostatic charge/discharge curves of the micro-supercapacitor at 1 A g^{-1}. (a–d) Reproduced with permission from ref. 132. Copyright 2013 WILEY-VCH Verlag GmbH & Co. KGaA, Weinheim. (e) Schematic illustration of a wire-shaped supercapacitor fabricated from two twined GF@3D-Gs with polyelectrolyte. (f) Photos of the textile embedded with two GF@3D-G fiber supercapacitors (*ca.* 2 cm in length for each of them) in flat and bending state, respectively. (g) CV curves of two GF@3D-G fiber supercapacitors as the textile in flat (f1) and bending (f2) states with a scan rate of 50 mV s^{-1}. (e–g) Reproduced with permission from ref. 139. Copyright 2013 WILEY-VCH Verlag GmbH & Co. KGaA, Weinheim.

3.2. Graphene

Graphene is composed of a single layer of hexagonally arranged sp^2 hybridized carbon atoms. Its unprecedented physical and chemical properties such as superior electronic conductivity, thermal conductivity, mechanical and chemical stability, unique two-dimensional (2D) morphology and ultrahigh surface area (2630 m^2 g^{-1})[127–132] forecast its enticing potential as a significant material for flexible SCs. Niu *et al.*[132] developed all-solid-state flexible ultrathin micro-supercapacitors (Fig. 4a and b) based on lateral ultrathin reduced graphene oxide (rGO) interdigitated microelectrodes on a polyethylene terephthalate (PET) substrate. The Au electrode acts as the current collector and the phosphoric acid/polyvinyl alcohol (H_3PO_4/PVA) gel serves as the electrolyte. These ultrathin rGO micro-patterned electrodes enhanced the ability of the H_3PO_4/PVA gel to infiltrate into the layers of rGO micro-patterned electrodes due to the shortened diffusion path lengths, leading to more effective utilization of the electrochemical surface area of graphene layers. The resulting devices achieved a much higher specific capacitance (Fig. 4c) of 285 F g^{-1} than conventional SCs (86 F g^{-1}). Furthermore, the columbic efficiency is nearly 98%, resulting from the perfectly linear charge/discharge curve (Fig. 4d) of the obtained micro-supercapacitor at a constant current of 1 A g^{-1}.

The strong π–π interaction between each component always leads to the aggregation of graphene nanosheets, thus the claimed large surface area cannot be fully utilized.[133] To overcome the over-stacking problem of graphene sheets, three-dimensional (3D) porous graphene has been developed to make high performance supercapacitors.[134–138] As illustrated in Fig. 4e, Meng *et al.*[139] fabricated a unique all-graphene core-sheath fiber-based electrochemical supercapacitor in which a core of flexible graphene fiber (GF) is covered with a sheath of 3D graphene network (denoted as GF@3D-G). The flexible GF is synthesized by integrating the graphene sheets into macroscopic ensembles, which possess the common mechanical flexibility characteristics of a fiber. As a result, the assembled fiber SCs can be conveniently woven into textile for wearable electronics (Fig. 4f and g). A specific capacitance of 30–40 μF g^{-1} is obtained even under cycling bending and releasing for 500 cycles.

3.3. Pseudo-capacitors

Generally, a SC is divided into an electrical double-layer capacitor (EDLC) and a pseudo-capacitor according to the charge storage mechanism. Typically, the capacitance of an EDLC comes from the pure electrostatic charge accumulated at the electrode/electrolyte interface, which is strongly dependent on the effective surface area of the electrode materials that is accessible to the electrolyte ions. Therefore, various carbon-based materials with high surface area such as active carbon, carbon particles, CNTs, graphene and their composites are most widely used as EDLCs. Pseudo-capacitors, on the other hand, use fast and reversible faradic processes of the redox-active materials based on transitional metal oxides as well as electronically conducting polymers for charge storage. Pseudo-capacitors have been extensively studied in the past few decades because their specific capacitance far exceeds that of EDLCs.[140–143] Yang *et al.*[144] reported edge-oriented MoS_2 thin films grown on Mo substrates serving as a flexible electrode with a high area capacitance of 12.5 mF cm^{-2} (Fig. 5a and b). Among the metal oxides, MnO_2 has been widely recognized as one of the most attractive electrode materials for SCs in terms of its high theoretical specific capacitance (1400 F g^{-1}), low cost, natural abundance, and environmental compatibility.[145] Lu *et al.*[146] fabricated a solid-

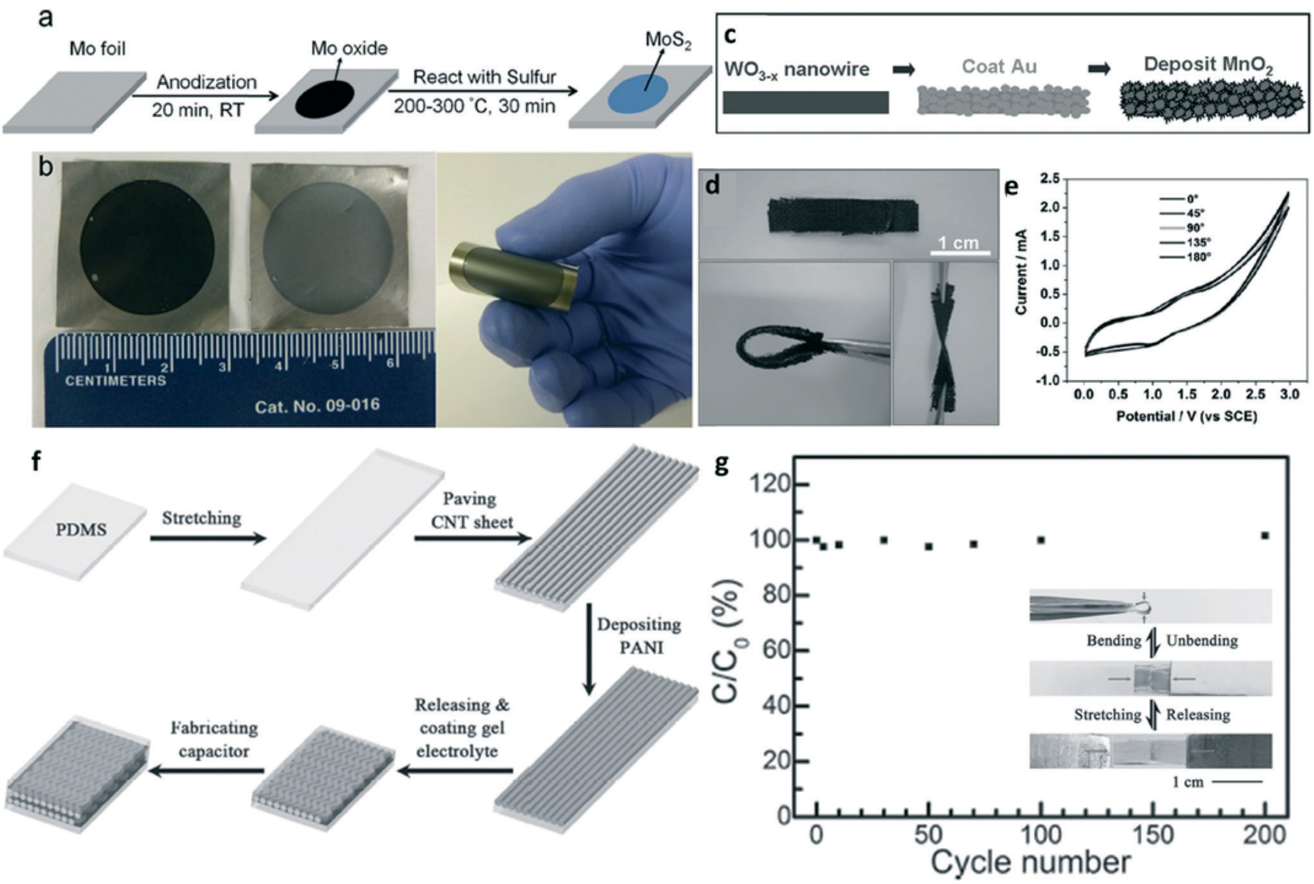

Fig. 5 (a) Schematic of the fabrication process and photographs of the flexible electrodes of the edge-oriented MoS_2 film. (b) Photographs of the flexible electrodes. The left photograph shows the visible difference between the Mo oxide (dark color) and MoS_2 (gray color). The right photograph shows the flexibility of the edge-oriented MoS_2 film. (a, b) Reproduced with permission from ref. 144. Copyright 2014 WILEY-VCH Verlag GmbH & Co. KGaA, Weinheim. (c) Schematic of the fabrication process for WO_{3-x}@Au@MnO_2 NWs. (d) Optical photographs of the as-fabricated solid-state supercapacitor device. The bottom images demonstrate the high flexibility of the as-prepared device. (e) CV curves of a WO_{3-x}@Au@MnO_2 supercapacitor at different curvatures of 0°, 45°, 90°, 135°, and 180° between 0 and 3 V. (c–e) Reproduced with permission from ref. 146. Copyright 2012 WILEY-VCH Verlag GmbH & Co. KGaA, Weinheim. (f) Schematic illustration of the fabrication of the smart supercapacitor of the PANI/CNTs films. (g) Dependence of specific capacitance on stretched cycle number at a strain of 100%. C_0 and C correspond to the specific capacitances before and after bending or stretching, respectively. The inset shows the photographs of a supercapacitor before and after bending and stretching. (f, g) Reproduced with permission from ref. 154. Copyright 2014 WILEY-VCH Verlag GmbH & Co. KGaA, Weinheim.

state SC with high flexibility by using hybrid WO_{3-x}@Au@MnO_2 core–shell nanowires (NWs) on flexible carbon fabric as electrodes (Fig. 5c). The flexible device can operate under bending conditions even at an angle of 180° without significant electrochemical performance degradation (Fig. 5d and e). By this way, the as-synthesized pseudo-capacitor overcomes the intrinsic low mass loading of MnO_2, resulting in a high specific capacitance of 1195 F g^{-1} at a current density of 0.75 A g^{-1}. Furthermore, the as-fabricated supercapacitor exhibits excellent long-term cycling stability, high power density (30.6 kW kg^{-1}) and energy density (106.4 W h kg^{-1}).

3.4. Conducting polymers

Conducting polymers have attracted significant research interest as flexible SCs due to their relatively high theoretical capacities ranging from 100 to 140 mA h g^{-1}.[147,148] The advantages of environmental compatibility, wide voltage window, remarkable storage capacity/reversibility, and adjustable redox activity also contribute to the wide attention.[149–153] The widely investigated conducting polymers including polypyrrole (PPy), polyaniline (PANI) and polythiophene (PTP) are promising candidates for manufacturing smart flexible SCs. It has been reported that some of the conducting polymers are sensitive to external environmental stimuli including temperature, pH, ion strength, solvent, and ligand interaction.[155,156] Different stimuli conditions can induce different colors, making them highly suitable as electrode materials for SCs and other smart energy devices. For example, Chen *et al.*[154] developed smart SCs by depositing the conducting polymer polyaniline (PANI) onto aligned CNT sheet electrodes (Fig. 5f). The capacitance achieved was 308.4 F g^{-1} and the SCs can be operated at a strain of up to 100% for 200 cycles (Fig. 5g). The color change can be immediately observed by our naked eyes at the same time during the stretching and recovering.

However, direct utilization of bulk conducting polymers as electrode materials suffered from a limited stability during cycling and caused electrochemical performance fading.[147,157,158] Thus, research efforts with conducting polymers for supercapacitor applications are nowadays developed towards their hybrid composites with various types of carbon materials with high stability.

3.5. Composites

Pure carbon material based flexible SCs usually exhibit high power density but relatively low energy density and specific capacitance arising from the limited charge accumulation on the electrode surface.[159,160] While pseudo-capacitance resulting from the fast and reversible faradic process of redox-active materials may provide much higher specific capacitances and energy density.[92] For developing high-capacitance supercapacitors, the composite electrodes which consist of carbon materials and pseudocapacitive active components have received great interest due to their significant improvements in both energy density and power density. Choi *et al.*[161] reported a MWNT/MnO_2 composite yarn supercapacitor obtained by depositing MnO_2 onto a multi-walled carbon nanotube (MWNT) yarn which is synthesized by twisting MWNT sheets. The micrometer diameter yarn electrode simultaneously served as the conductive pathway, flexible substrate and current collector. Effective electron delivery between the active material MnO_2 and uniaxial aligned CNT bundles of yarn is realized, resulting in a high specific capacitance value of 25.4 F cm^{-3} (Fig. 6a), energy and average power densities (3.52 mW h cm^{-3} and 127 mW cm^{-3}, respectively). Because of the mechanical flexibility properties of the composite yarn electrodes, there was no significant capacitance drop even after the 1000th bending cycle at a bending angle of 90° (Fig. 6c). Furthermore, the flexible yarn electrode was woven into commercial textile for application as a smart cloth (Fig. 6b). Other than the commonly used electrochemical active materials, a MOF is another choice to serve as a supercapacitor electrode. Cao *et al.*[162] reported a flexible electrode material (Fig. 6d and e) obtained by wrapping porous reduced graphene oxide (rGO) onto Mo containing MOF derived MoO_3. They fabricated all-solid-state, flexible supercapacitor devices by using a rGO/MoO_3 composite as the electrode, a Au film-coated poly(ethylene terephthalate) (PET) substrate as the flexible current collector, and a H_2SO_4/poly(vinyl alcohol) (PVA) gel electrolyte as the solid electrolyte. The device showed a capacitance retention of 80% after 5000 cycles at a high current density of 2 A g^{-1} (Fig. 6f) and a maximum energy density of 14 W h kg^{-1} at a power density of 500 W kg^{-1}. Owing to its large specific capacitance (1340 F g^{-1}), high electrical conductivity and suitable working window, vanadium nitride (VN) is considered as a promising pseudo-capacitive candidate for next-generation high performance SCs.[163] Xiao *et al.*[164] designed a high performance all-solid-state flexible SC with flexible freestanding mesoporous VN nanowires (MVNNs)/CNT hybrid electrodes. The whole weight of the device (including the electrodes, separator and electrolyte) was only 15 mg, resulting in a high volume capacitance of 7.9 F cm^{-3}.

Hybrid composites based on conducting polymers and carbon materials have also been extensively studied as flexible SCs. Yu *et al.*[165] developed a solid-state supercapacitor device with remarkable flexibility, which could be stretched to a large strain of 50% without decreasing its conductivity. The device was assembled by depositing a layer of polyaniline (PANI) nanofibers on the water surface assisted synthesized MWCNT/PDMS film to form the PANI/MWCNT/PDMS film electrode. The electrode exhibited a benchmark specific gravimetric capacitance of 1023 F g^{-1} and an area capacitance of 481 mF cm^{-2} at a scan rate of 5 mV s^{-1}. Moreover, the as-fabricated SC exhibited 95% capacitance retention after 500 cycles during the dynamic stretching and releasing process. And the maximum energy density of the device is 0.15 mW h cm^{-3} (11 W h kg^{-1}) at a current density of 2 mA cm^{-2}. Recently, a similar super-elastic supercapacitor based on two aligned carbon nanotube (CNT)/polyaniline (PANI) composite sheets was designed by Zhang *et al.*[44] It can be stretched to a large strain of 400% without performance degradation. As illustrated in Fig. 7, a relatively high specific capacitance of approximately 79.4 F g^{-1} is well maintained after stretching at a

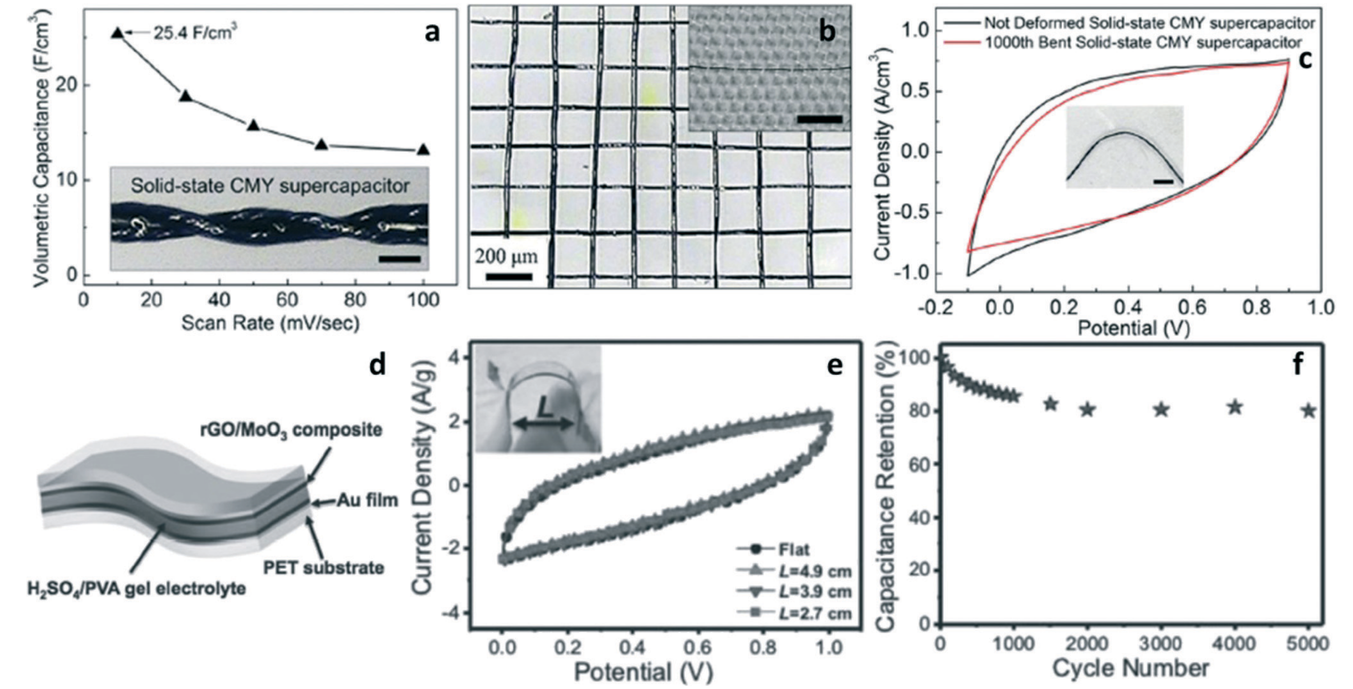

Fig. 6 (a) Volumetric capacitance of all-solid-state CMY electrode as a function of scan rate. (b) Optical image of hand-made CMY textile consisting of 15 yarns. Inset: A CMY electrode woven into a commercial textile (scale bar represents 1 mm). (c) Comparison of CV plots of solid-state CMY supercapacitor before and after the 1000th bending test. (a–c) Reproduced with permission from ref. 161. Copyright 2013 WILEY-VCH Verlag GmbH & Co. KGaA, Weinheim. (d) Schematic illustration of the configuration of the all-solid-state flexible supercapacitor device fabricated with rGO/MoO_3 composite. (e) CV curves of the device under different bending status. Inset: Photograph of a bent device (L = 4.3 cm). (f) Cycling performance measured by charging and discharging the device at 2 A g^{-1} for 5000 cycles. (d–f) Reproduced with permission from ref. 162. Copyright 2015 Wiley-VCH Verlag GmbH & Co. KGaA, Weinheim.

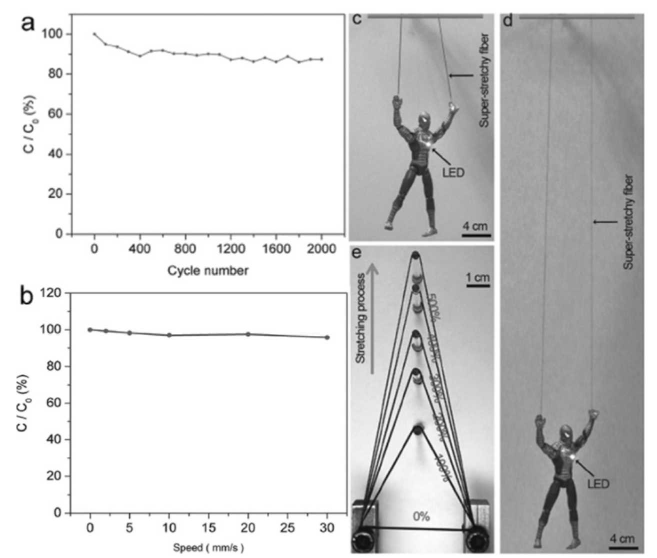

Fig. 7 (a) Dependence of specific capacitance on cycle number of CNT/PANI elastic fiber electrodes at a current density of 1 A g^{-1}. (b) Dependence of specific capacitance on stretching speed of CNT/PANI elastic fiber electrodes. C_0 and C correspond to specific capacitances at 0 and the other strain, respectively. (c, d) Photographs of the elastic fiber electrode used to power a light emission diode before and after stretching by a load, respectively. (e) Photograph of an elastic fiber electrode before and after stretching by 100%, 200%, 300%, 400%, and 500%. (a–e) Reproduced with permission from ref. 44. Copyright 2014 WILEY-VCH Verlag GmbH & Co. KGaA, Weinheim.

strain of 300% for 5000 cycles and 100.8 F g^{-1} after bending for 5000 cycles at a current density of 1 A g^{-1}. The specific capacitance of the flexible SCs can be maintained by 95.8% at a stretching speed as high as 30 mm s^{-1}. To achieve the development of flexible electrodes for SCs with different configurations, Liu *et al.*[166] coated the microscale porous reduced graphene oxide (rGO)/cellulose fiber (rGO/CF) composite paper with PANI to develop two kinds of SCs with a compact design and nanostructured configuration. A high specific capacitance of 464 F g^{-1} is achieved for the PANI-rGO/CF composite paper when used as a supercapacitor electrode.

4. Strategies to improve the performance of supercapacitors

4.1. Asymmetric SCs

Besides improving the specific capacitance of the electrode, the energy density (E) of flexible SCs can also be increased by maximizing the cell voltage (V) according to the equation: $E = 0.5CV^2$.[167] For this purpose, a promising strategy is to develop an all-solid-state asymmetric SC by coupling different positive and negative electrode materials with well-separated potential windows to obtain a high operation voltage. Typically, nanostructured carbon-containing materials were used as Faradic electrodes (energy source) and a suitable carbon material served as the capacitance electrode (power source).

Such a device can effectively make use of the different potential windows of the two electrodes to provide a maximum operation voltage up to 2 V, and hence significantly enhance the device energy density.[167] Chen *et al.*[168] constructed an asymmetric SC (Fig. 8a) containing a 3D bacterial cellulose pellicle (p-BC) nanofiber network coated MnO_2 (p-BC@MnO_2) as the positive electrode and a nitrogen-doped p-BC (p-BC/N) nanomaterial as the negative electrode. The optimized device can be reversibly charged/discharged at a potential window of 2.0 V (Fig. 8b) in an aqueous electrolyte, reaching a considerably high energy density of 32.91 W h kg^{-1} and a maximum power density of 284.63 kW kg^{-1}. Meanwhile, the hybrid supercapacitor exhibits good cycling stability with 95.4% specific capacitance retention after 2000 cycles.

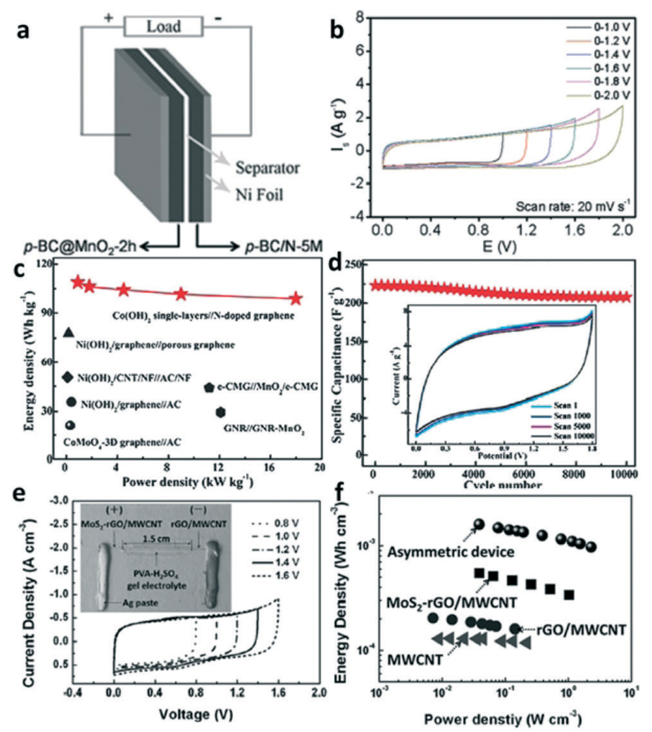

Fig. 8 (a) Scheme of the asymmetric supercapacitor (p-BC@MnO_2-2 h//p-BC/N-5 M) with p-BC@MnO_2-2 h as the positive electrode and p-BC/N-5 M as the negative electrode in 1.0 M Na_2SO_4 aqueous electrolyte. (b) CV curves of different operation voltages at a scan rate of 20 mV s^{-1}. (a, b) Reproduced with permission from ref. 168. Copyright 2013 WILEY-VCH Verlag GmbH & Co. KGaA, Weinheim. (c) Electrochemical performance of the single-layer β-$Co(OH)_2$ all-solid-state asymmetric supercapacitor in comparison with previously reported asymmetric supercapacitors. (d) Cycle performance of the single-layer β-$Co(OH)_2$ all-solid-state asymmetric supercapacitor measured at a scan rate of 20 mV s^{-1}; the inset shows the corresponding CV curves. (c, d) Reproduced with permission from ref. 168. Copyright 2014 Wiley-VCH Verlag GmbH & Co. KGaA, Weinheim. (e) CV curves of rGO/MWCNT fiber and MoS_2-rGO/MWCNT fiber based asymmetric supercapacitors at cell voltages of 0.8, 1, 1.2, 1.4, and 1.6 V. Inset: Optical image of a fiber-based asymmetric supercapacitor on glass slide. (f) Plot of energy density *versus* power density for fiber-based asymmetric supercapacitor and those of MoS_2-rGO/MWCNT, rGO/MWCNT, and bare MWCNT fiber-based symmetric supercapacitors. (e, f) Reproduced with permission from ref. 174. Copyright 2015 Wiley-VCH Verlag GmbH & Co. KGaA, Weinheim.

To improve the specific capacitance, various materials, such as metal hydroxides, have been investigated as cathodes in asymmetric supercapacitors.[24,169] Among them, β-$Co(OH)_2$ is one of the most promising candidates owing to its high theoretical capacitance of 3460 F g^{-1} and natural abundance.[170] Gao *et al.*[167] fabricated a novel cathode with β-$Co(OH)_2$ single layers with a five-atom layer thickness. This kind of structure not only features a shorter ion diffusion path but also provides 100% exposed hydrogen atoms to serve as the electroactive sites, thus favoring Faradic redox reactions. Benefiting from these features, an all-solid-state asymmetric supercapacitor fabricated from single-layer β-$Co(OH)_2$ as the cathode and N-doped graphene as the anode displayed a high energy density of 98.9 W h kg^{-1} at an exceptional power density (Fig. 8c) of 17 981 W kg^{-1}, which is comparable to that of lithium-ion batteries. Furthermore, this integrated asymmetric supercapacitor achieves an excellent cycling life and a 93.2% capacity retention after 10 000 charge/discharge cycles (Fig. 8d). Owing to their unique electrochemical properties, two dimensional (2D) nanosheets of transition-metal dichalcogenides (TMDs, particularly MoS_2)[171,172] have been shown to be attractive anodes for asymmetric SCs.[173] Recently, Sun *et al.*[174] incorporated MoS_2 and reduced graphene oxide (rGO) nanosheets into MWCNT fibers to fabricate solid-state, asymmetric supercapacitors (Fig. 8e) by using MoS_2-rGO/MWCNT and rGO/MWCNT fibers as the anode and cathode, respectively. The resulting extremely flexible asymmetric supercapacitor demonstrates a much higher energy density and power density than symmetric SCs and can be operated in a wide potential window of 1.4 V (Fig. 8f). Furthermore, both the volumetric capacitance and coulombic efficiency are steady even under repeated bending for 7000 cycles.

4.2. Series SCs

In general, the working potential window and energy storage capacity of a single SC is limited to meet practical applications. As a result, assembling several SCs in series, or in parallel, into one integrated unit would be a simple and viable way to improve the overall output potential and current. As a proof of concept, Niu *et al.*[175] integrated four highly compressible all-solid-state SCs (Fig. 9a–d) into one unit in series by using PANI-SWNT sponge as electrodes, PVA/H_2SO_4 as a solid electrolyte, Au films on poly(ethylene terephthalate) (PET) substrates as current collectors, and filter paper as a separator. This resulting integrated SC unit was powerful enough to light up a red light-emitting diode (LED) when fully charged and displayed a good compression tolerant ability (Fig. 9e–h). The CV curve of such four devices in series exhibited an enhanced potential range of 0–3.2 V, which is four times that of a single supercapacitor (Fig. 9i). It is also reflected by the charge/discharge curve, where the charge potential can reach up to 3.2 V (Fig. 9j). For eliminating inactive ingredients such as binders and current collectors, Xiao *et al.*[164] fabricated flexible freestanding mesoporous VN nanowires (MVNNs)/CNT hybrid electrodes and obtained high

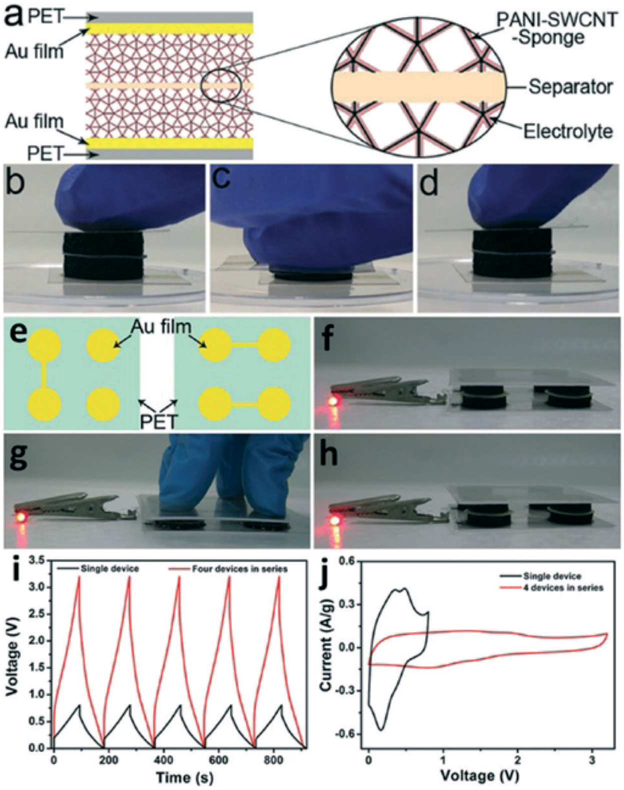

Fig. 9 (a) Schematic diagram of an all-solid-state integrated supercapacitor based on PANI–SWCNTs–sponge. (b–d) Real-time optical images of a supercapacitor showing the compressing and recovering process. (e) Au film patterns on PET substrates for assembling four supercapacitors into one unit in series. (f–h) Real-time optical images of the resulting four-supercapacitor group showing the compressing and recovering process. The galvanostatic charge/discharge curves of the four-supercapacitor group and a single supercapacitor at 0.4 A g^{-1}. (i) The CV curves of the four-supercapacitor group and a single supercapacitor at a scan rate of 5 mV s^{-1}. (j) The charge/discharge curve of the four-supercapacitor group and a single supercapacitor. (a–j) Reproduced with permission from ref. 175. Copyright 2015 WILEY-VCH Verlag GmbH & Co. KGaA, Weinheim.

performance all-solid-state flexible SCs. Three devices were connected in series or parallel to test the galvanostatic charge/discharge curves at the same current (0.5 mA). The three devices connected in series exhibited a charge/discharge voltage of 2.1 V with almost the same discharge time as a single device. Furthermore, the discharge time of the three devices connected in parallel was about 2.5 times larger than that of a single device, which approached the theoretical factor 3, confirming to the theorem of series and parallel connections of capacitors. To demonstrate the flexibility and foldability of the series SCs, Liu *et al.*[166] prepared four SC units based on PANI-rGO/CF composite paper in series to light a red LED. The all-solid-state SCs could stably light the LED when they were twisted and folded simultaneously, which have potential applications in future wearable or printable electronics.

4.3. Micro-SCs

Current research on SCs has focused on their applications for portable/wearable electronics, which stimulated the development of miniaturized energy storage devices. As one type of newly developed miniaturized electrochemical energy-storage devices, micro-SCs can offer power densities that are much larger than those of conventional batteries and SCs because of their fast responses to ions and electrons.[176] Besides, miniaturized energy storage devices integrated into a chip would potentially increase the density of devices with different functionalities and reduce overall chip design complexity by eliminating intricate interconnects in bulk-sized energy storage devices.[177] Recent work has illustrated that high performance micro-scale SCs can be fabricated onto a chip using different active materials and designs, such as CNTs, graphene sheets, activated carbons, and conductive polymers.[178–187] Meng *et al.*[176] fabricated an ultrathin flexible all-solid-state SC (Fig. 10b) based on a leaf formed nanocomposite structure of polypyrrole (PPy)-decorated nanoporous gold (NPG) as both the electrode support and current collector (Fig. 10a). The total thickness of the supercapacitor is less than one micrometer. Because of the fast responses to ions and electrons, this symmetric SC thus produced a large specific capacitance (270 F g^{-1}) at a current density of 0.6 A g^{-1}. And it showed a power density of 296 kW kg^{-1}, an energy density of 27 W h kg^{-1}, and exhibited almost identical performance at various curvatures (Fig. 10c–g), suggesting its wide application potential in powering wearable/miniaturized electronics.

Continuous carbon nanotube yarn can be fabricated by means of dry and wet spinning methods, which greatly promotes the development of fiber shaped micro-supercapacitors. Meng *et al.*[188] developed a high-performance yarn micro-supercapacitor with single-walled carbon nanotubes and activated carbon electrodes. The combination of single-walled carbon nanotubes and activated carbon provides the yarn micro-supercapacitors with more effective area for ion transportation and energy storage. The specific volumetric capacitance reaches 48.5 F cm^{-3}, corresponding to a gravimetric capacitance of 74.6 F g^{-1} at a scan rate of 2 mV s^{-1}. Besides,

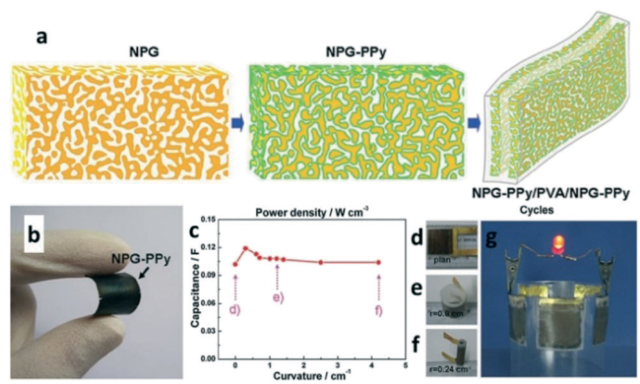

Fig. 10 (a) Schematic illustration of the fabrication process of the ultrathin NPG-PPy/PVA/NPG-PPy flexible solid state supercapacitor. (b) Digital pictures of macroscopic NPG-PPy thin membrane. (c) Response of a single NPG-PPy_{120s} supercapacitor at different curvatures from 0 to 4 cm^{-1}. (d–f) Digital images of an all-solid-state supercapacitor device at different bending states. (g) LED lighting demonstration, powered by three pieces of supercapacitors in series. (a–g) Reproduced with permission from ref. 176. Copyright 2011 WILEY-VCH Verlag GmbH & Co. KGaA, Weinheim.

the energy density is 3.7 mW h cm^{-3} at a power density of 45.7 mW cm^{-3}. The device shows high stability with a capacitance retention of 98.5% after 10 000 charge–discharge cycles. Such four micro-supercapacitors with high capacitance, energy density and cycling stability were also connected together in parallel and in series configurations (Fig. 11a–d), thus the current and potential range of the yarn micro-SCs were enlarged. Different from the planar micro-SCs on one-chip, flexible fiber-shaped SCs show incomparable advantages that they can be directly used as flexible, wearable and embedded device units.[163] Sun *et al.*[189] synthesized graphene/CNT composite fibers to fabricate a wire-shaped micro-SC with a specific capacitance of up to 31.50 F g^{-1} (4.97 mF cm^{-2} or 27.1 μF cm^{-1}), much higher than that of a bare CNT fiber based supercapacitor (5.83 F g^{-1}, 0.90 cm^{-2} or 5.1 μF cm^{-1}) under the same testing conditions. Moreover, the graphene/CNT composite fibers were flexible and tough, and they could be easily woven into a piece of cotton fabric. Two composite fibers served as conducting wires to connect a blue light emitting diode (LED) lamp with a direct-current power (Fig. 11e and f). The lamp could be stably operated without any fatigue in the illumination after 5000 bending cycles.

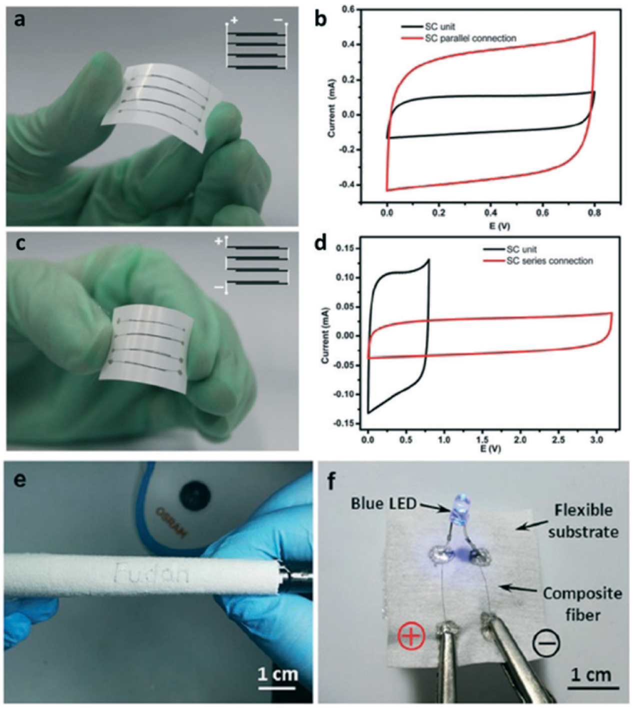

Fig. 11 (a–d) The electrochemical performance of the yarn micro-supercapacitors in series and parallel. (a) Four units in parallel (insert image is the parallel connection diagram of supercapacitors). (b) Cyclic voltammograms of the unit and parallel circuit. (c) Four units in series (insert image is the in series connection diagram of supercapacitors). (d) Cyclic voltammograms of the unit and in series circuit. (a–d) Reproduced with permission from ref. 188. Copyright 2014 WILEY-VCH Verlag GmbH & Co. KGaA, Weinheim. (e) Photographs of graphene/CNT composite fibers being woven into a flexible cotton fabric to make up the word "Fudan". The inserted image shows the "F" at a higher magnification. (f) Photographs of a blue light emission diode lamp connected to a direct-current circuit with two graphene/CNT composite fibers with length of ~1.5 cm as conducting wires. The voltage was set to 3 V. (e, f) Reproduced with permission from ref. 189. Copyright 2014 WILEY-VCH Verlag GmbH & Co. KGaA, Weinheim.

As shown in Fig. 12, micro SCs have a relatively higher power density compared with other SCs. Also, it is clearly seen that the energy density is inferior to those of other reported SCs because of the miniaturized structure. It is hopeful to improve the supercapacitor performance by developing a complex and optimized structure, enlarging the stack density or surface area. Alternatively, the performance of the micro SCs can be improved by controlling the composition of the hierarchical nanomaterials as electrodes and ionic liquid or organic based polymers as electrolytes, and optimizing the electrode pattern into interdigitated 2D microscale or semi-3D devices. Another promising approach is to directly integrate or couple micro SCs with micro-batteries to achieve high energy and power densities. Moreover, there is great hope that integration of green materials such as biomaterials and new functions could further expand their applications for the fabrication of green micro SCs. Thus as one type of newly developed miniaturized electrochemical energy-storage devices, micro-SCs can offer several orders of magnitude higher power density than conventional SCs, long cycle life and large rate capability, and they are environmentally-friendly as well.

4.4. Electrolytes

In spite of the electrode materials that significantly influence the SC performance, the electrolyte is another important factor that should be considered to obtain high performance SCs. Specifically, the electrolyte involves liquid and solid-state forms. Because a liquid electrolyte based SC configuration suffers from possible leakage of harmful electrolytes and undesired dislocation of the electrode position during stretching, solid-state electrolytes are preferred in flexible SCs owing to their advantages in terms of compactness, reliability, and freedom from leakage.[86,174,188]

Gel electrolytes are actually quasi-solid-state electrolytes which are composed of a polymeric framework, an organic/

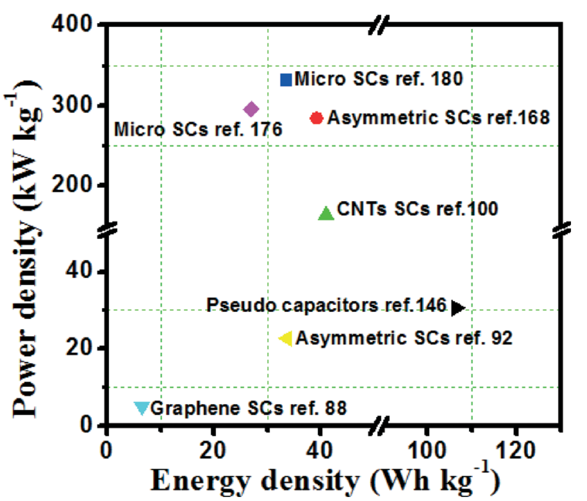

Fig. 12 Energy and power densities of various SCs.

aqueous solvent as the dispersion medium and a supporting electrolytic salt/acid/alkali. They possess high physical flexibility, desirable electrochemical properties, excellent mechanical integrity and high ionic conductivity of $\sim 10^{-4}$ to 10^{-1} S cm^{-1} under ambient conditions.[192] However, most hydrogel polymer electrolytes which were employed in flexible SCs, such as PVA-H_2SO_4 and H_3PO_4 systems, are merely a blended solution which usually cause harm to the structural integrity and mechanical strength.[56,193] To address this problem, Wang *et al.*[194] synthesized a chemically crosslinked PVA-H_2SO_4 hydrogel film, which differs from the laminated configuration of conventional SCs. The conducting PANI was *in situ* embedded in the PVA-H_2SO_4 hydrogel film to serve as electrode materials, constructing an integrated flexible SC. With this novel configuration, the prototype-integrated SC can sustain up to 300% stretching and a large areal capacitance (488 mF cm^{-2}) is obtained at the same time.

Ionic liquids, which are known as room temperature molten salts, are attractive candidates for electrolytes in flexible SCs because of their high conductivity, semi-solid state, thermal stability and flexiblity.[195] Balducci *et al.*[196] reported that using carbide derived carbon as an electrode material and EMI/TFSI ionic liquid (EMI = 1-ethyl-3-methylimidazolium, TFSI= bis(trifluoromethanesulfonyl)imide) as an electrolyte, a high capacitance of 160 F g^{-1} was obtained at 60 °C and the cell voltage can be extended to 3.5 V. However, current ionic conducting gels are brittle and cannot exhibit pressure-dependent performance in energy storage devices. Liu *et al.*[197] prepared a self-healing hydrogel system which consists of four components: 1-ethyl-3-methylimidazolium chloride (EMIMCl), hydroxyethyl methacrylate (HEMA), chitosan (CS) and water. The specific electrode capacitance can be tuned by compressive pressure, which demonstrated a significant improvement in the specific capacitance from 43 F g^{-1} to 98 F g^{-1} with the strain less than 20%, and then increased to 134 F g^{-1} with a slightly lower rate. This pressure-dependent electrochemical property is due to the supramolecular structure of these materials, which makes them quite suitable for versatile flexible energy devices and platforms for pressure sensors.

5. Outlook and future challenges

The prospect of flexible supercapacitors

Integrated systems which could be stretched or folded as an integrated unit have been developed extensively in recent years because they overcame the limitation of the conventional stretchable SC configuration wherein two electrodes have to move relative to the separator under strains[13] (Fig. 13). All-solid-state integrated SCs are favored over their liquid counterparts for the consideration of encapsulation and safety since it is possible for them to avoid the leakage of harmful electrolytes and undesired dislocation of the electrode position during stretching.[198] Niu *et al.*[13] achieved highly stretchable integrated supercapacitors by using SWCNT films as electrodes and H_2SO_4-polyvinyl alcohol (PVA) gel as both the electrolyte and separator. The as-prepared stretchable supercapacitor exhibits nearly stable performance even under the strain of 120%, which is remarkably larger than other stretchable batteries and supercapacitors with conventional structures. Liu *et al.*[166] also fabricated another kind of all-solid-state integrated SC based on PANI-rGO/CF composite paper. The calculated specific capacitance of the composite paper is about 224 F g^{-1}, and the paper capacitor maintained a value of 89% with respect to the maximum capacity after 1000 cycles. There was only a very slight difference in the CV curves when the composite paper was rolled up and folded, indicating a good recycling stability.

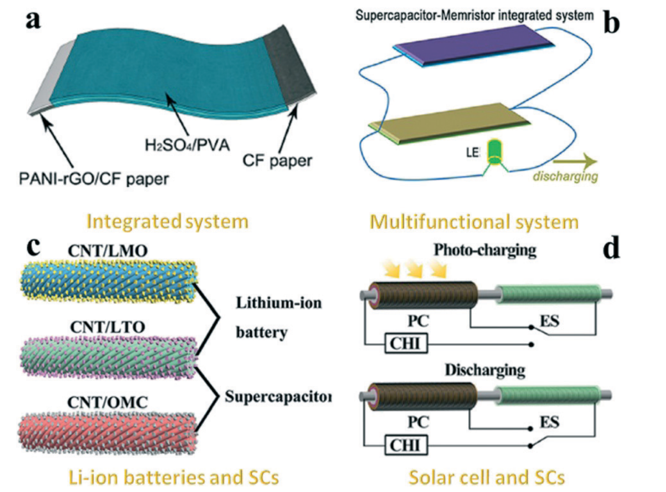

Fig. 13 Prospect of flexible supercapacitors: (a) integrated system. Reproduced with permission from ref. 166. Copyright 2014 WILEY-VCH Verlag GmbH & Co. KGaA, Weinheim. (b) Multifunctional system. Reproduced with permission from ref. 191. Copyright 2014 WILEY-VCH Verlag GmbH & Co. KGaA, Weinheim. (c) Lithium-ion battery and SCs. Reproduced with permission from ref. 207. Copyright 2015 Wiley-VCH Verlag GmbH & Co. KGaA, Weinheim. (d) Solar cell and SCs. Reproduced with permission from ref. 208. Copyright 2013 WILEY-VCH Verlag GmbH & Co. KGaA, Weinheim.

One drawback associated with supercapacitors is that their voltage often significantly decreases once they begin to discharge as power sources, which greatly affects the smooth operation of the electronic/optoelectronic devices.[190,191] To achieve a voltage-stabilizing supercapacitor system, Liu *et al.*[191] integrated a SnO_2-based memristor (which is the fourth circuit element and has observable effects in resistance switching memory) with a PCBM-based supercapacitor to design a novel M-S integrated device. When it was charged to 1 V, a stable discharging curve is obtained for the integrated device at about 0.8 V for as long as 200 s, while only about 0.11 V potential drop was observed. Meanwhile for a single supercapacitor, once discharging, the voltage drops dramatically from 0.86 V to 0.3 V within the measured discharging time (200 s). Importantly, to demonstrate the real application of the integrated M–S system as stabilized energy units, they also attempted to control a commercial red LED by using the as-designed M–S system. For a single supercapacitor, it can be observed that the brightness of a lighted LED decreased very fast and then fully disappeared within 100 s during the continuous discharging process.

Meanwhile for the M–S integrated system with voltage-stabilizing ability, the LED was found to be still lighted after 100 s, confirming the voltage stabilizing features of the memristor–supercapacitor system.

Recently, a great demand for high-performance multifunctional integrated systems has arisen because of the maximum functionality of these integrated systems with respect to conventional devices with a single function. Considerable research efforts have been made to integrate different functional units into single multifunctional systems such as integrated energy-storage devices, photodetector-supercapacitor nanosystems[198] and hydrogen generation-supercapacitors.[199] Chen *et al.*[156] developed a smart SC by depositing polyaniline (PANI) onto aligned CNT sheet electrodes, which can sense the level of stored energy and reflect the changes by chromatic transition between yellow, green and blue that can be directly observed by the naked eye (Fig. 14a). In this respect, it can be directly observed by the color changes to determine whether the energy has been consumed before a device stops working in practical applications. Recently, integrated photodetectors are of great importance due to their specific applications including environmental monitoring, biosensing and *in situ* monitoring of medical therapy.[200] Wang *et al.*[201] successfully prepared a microscale flexible asymmetric supercapacitor using Co_3O_4 nanowires on titanium wire as the positive electrode and graphene on carbon fibers as the negative electrode, forming a flexible energy-storage device and photodetector (Fig. 14b). This multifunctional system improved the energy storage and power delivery (at least by 1860%) by enlarging the potential window from 0–0.6 V to 0–1.5 V. In addition, the integrated flexible fiber-based asymmetric supercapacitor exhibits excellent response to white light.

The increasing energy and power requirement for next generation flexible electronics stimulates more and more efforts to explore new integrated devices to simultaneously realize energy conversion and storage that meet the critical requirement of being self-powered in the future.[202–206] However, how to realize both high energy and high power densities in one device still remains a challenge. Zhang *et al.*[207] fabricated a novel fiber-shaped hybrid energy storage device (FESD) by twisting CNT/ordered mesoporous carbon (OMC) and CNT/$Li_4Ti_5O_{12}$ (LTO) or CNT/$LiMn_2O_4$ (LMO) hybrid fibers together, resulting in an integrated system (Fig. 15a) with a lithium-ion battery (LIB) and SC to obtain both high energy and power densities. The LIB and supercapacitor segments can be effectively operated together to achieve a whole charge–discharge process (Fig. 15b and e). This fiber-based multifunctional device exhibited high power densities up to around 1 W cm^{-3} and a high energy density of 50 mW h cm^{-3}, which far exceeded the electrochemical

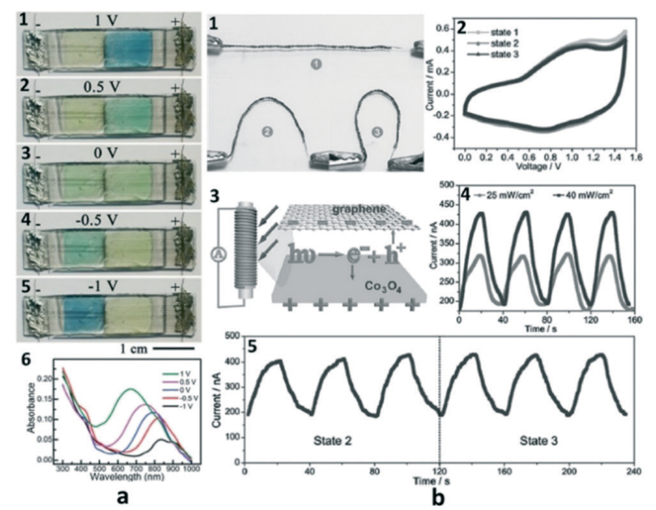

Fig. 14 (a) Reversible chromatic transition of a smart supercapacitor based PANI/CNT electrode during a charging–discharging process (a1–a5) from 1 V to −1 V and UV-vis spectra (a6) of the positive electrode corresponding to the states at (a1–a5). Reproduced with permission from ref. 156. Copyright 2014 WILEY-VCH Verlag GmbH & Co. KGaA, Weinheim. (b) Electrochemical performance of integrated asymmetric supercapacitor and the photodetector: (1) photographs of the fiber-based all-solid-state flexible asymmetric supercapacitor at different bending states; (2) CV curves obtained at a scan rate of 100 mV s^{-1} at different bending states; (3) schematic illustration of the integrated system. Current response of the photodetector powered by the flexible asymmetric fiber supercapacitor (4) illuminated under different incident light intensities, and (5) at different bending states under a light intensity of 40 mW cm^{-2}. Reproduced with permission from ref. 201. Copyright 2014 Wiley-VCH Verlag GmbH & Co. KGaA, Weinheim.

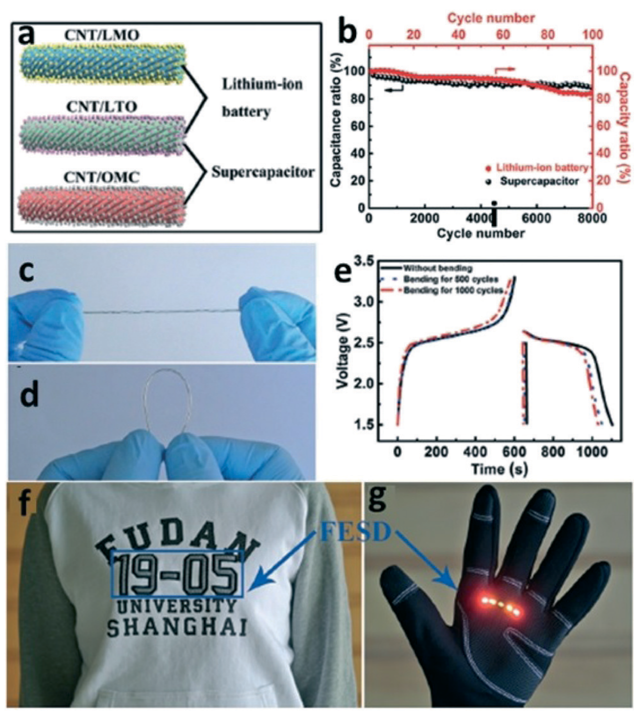

Fig. 15 (a) Schematic illustration of the constitution of the LIB and supercapacitor segments of the FESD. (b) Cyclic performance of the LIB and supercapacitor segments. (c, d) Photographs of an FESD before and after bending, respectively. (e) The charge and discharge curves of an FESD before and after bending for 500 and 1000 cycles. (f) Photograph of the FESD woven into a knitted sweater as the symbol "19-05". (g) Photograph of the FESD woven into a glove to power five light-emitting diodes. (a–g) Reproduced with permission from ref. 207. Copyright 2015 Wiley-VCH Verlag GmbH & Co. KGaA, Weinheim.

storage performance of other energy devices. Moreover, the devices were also wearable as they can be woven into various flexible textiles, such as a knitted sweater (Fig. 15f) and a glove (Fig. 15g). As a demonstration, the resulting glove can effective power five light-emitting diodes, indicating its potential for future wearable smart textiles. To simultaneously convert solar energy to electric storage energy, Zhang *et al.*[208] presented an integrated polymer solar cell and an electrochemical SC to a novel, all-solid-state, flexible "energy fiber" which can realize the functions of photovoltaic conversion (PC) and energy storage (ES) (Fig. 16b). This "energy fiber" (Fig. 16a) has also been realized on the basis of titania nanotube-modified Ti wires and aligned MWCNT sheets which served as two separate electrodes. The integrated system exhibits slight performance degradation (less than 10%) after bending for 1000 cycles (Fig. 16e), which opens a new avenue for future photoelectronics and electronics.

Table 1 shows the comparison of various SCs, which illustrates that flexible SCs based on EDLC materials (CNTs and graphene) possess higher power density but lower energy density and specific capacitances than those of pseudo-capacitors

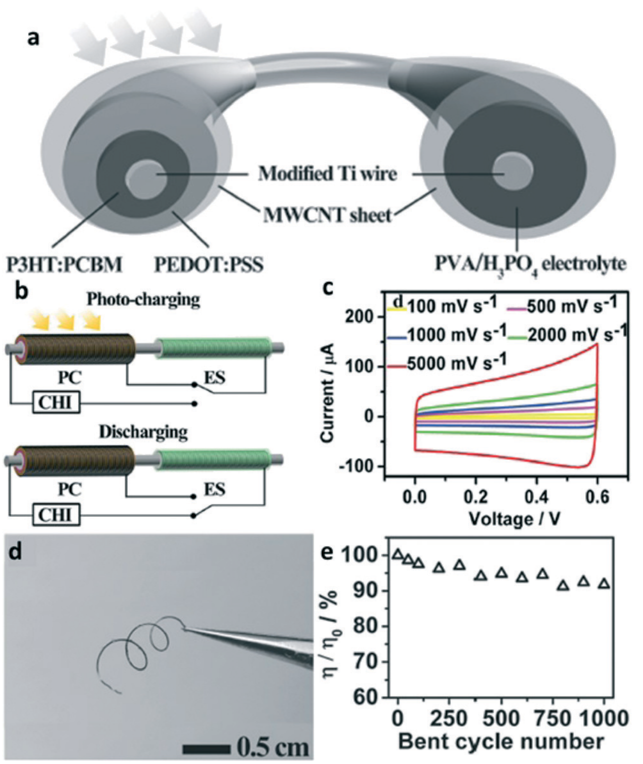

Fig. 16 (a) Schematic illustration of the structure of all-solid-state, coaxial and integrated fiber shaped device. The left and right sections correspond to the PC and ES parts, respectively. (b) Schematic diagram shows the circuit connection state in the process of charging and discharging. (c) Cyclic voltammograms at increasing scan rates from 100 to 5000 mV s^{-1}. (d) "Energy fibers" being bent into circles. (e) Change of the entire photoelectric conversion and storage efficiency of the "energy fiber" under bending for 1000 cycles. η_0 and η correspond to the entire efficiency before and after bending. (a–e) Reproduced with permission from ref. 208. Copyright 2013 WILEY-VCH Verlag GmbH & Co. KGaA, Weinheim.

Table 1 Comparison of the electrochemical performance of representative SCs

Material	Maximum power density (kW kg^{-1})	Maximum specific capacitances (F g^{-1})	Maximum energy density (W h kg^{-1})	Ref.
CNTs	164	135	41	100
Graphene	776.8	273.1	150.9	134
	5.0	186	6.5	88
Pseudo	30.6	1195	106.4	146
	3.75	145	16	141
Composites	500	404	14	162
Asymmetric	284.63	256.74	32.91	168
	22.7	560	33.71	92
Series	1.5	216	8	175
Micro	296	270	27	176
	332.5	946	53.4	180

resulting from their different charge storage mechanisms. Composite electrodes which were constituted by highly conductive carbon nanomaterials and pseudocapacitive materials as well as the asymmetric configuration derived from a Faradic electrode and capacitance electrode combined the advantages of both the two materials, which can achieve both high energy and power density. Series SCs assembled by several SCs together enlarged the working potential and current, making them more suitable to meet practical application. To meet the requirement for miniature devices, micro-SCs can provide short ion diffusion paths and high diffusion rates, resulting in higher power densities. Although a lot of electrode materials have been fabricated, the energy and power densities still need to be improved. Flexible integrated energy storage systems composed of flexible SCs and batteries could be a hopeful solution. Furthermore, the discovery of novel electrode materials with high specific surface area, short ion-transfer path and continuous pore network could also improve the overall performance of flexible SCs.

State-of-the-art SCs have achieved great advancements in recent years. Despite this, current wearable SCs are still far away from satisfying the requirements for wearable electronics, and much effort should be made to further improve them for practical applications. Although SCs exhibit high power densities, the energy density is the main obstacle for their widespread applications. Conducting polymers and metal oxides with high capacity have been combined with porous carbon nano-architectures to obtain high performance capacity electrodes. Optimizing the electrode architecture or cell configuration is an efficient strategy to obtain SCs with high energy density. Another alternative to improve the SC performance is developing hybrid energy storage systems. For example, the combination of a SC with a Li-ion battery results in an energy storage system with high power and energy densities. With the same energy consumption, in comparison with that of conventional electric devices, wearable SCs have the unique properties of being light weight, miniaturized and flexible. Wearable supercapacitors could be directly worn on the human body and work stably under complex deformation when they are used in practical applications, such as bending, folding and even stretching. To summarize, although many problems need to be addressed in flexible SCs in terms of material, structure and properties, they represent a new family of energy storage systems based on the excellent properties of being flexible and having fast charge–discharge abilities, which may change our life in the near future.

6. Conclusions

In this perspective, the most recent advances in smart, stretchable and wearable supercapacitors are summarized systematically, including flexible devices, various flexible electrode materials and the strategies to improve the performance of supercapacitors. An improved understanding of the current achievements in integrated and multifunctional systems has also been introduced to show the prospects of flexible supercapacitors. Although great progress has been made, many challenges still exist and need to be overcome. For instance, since each flexible electrode material has its own strength and shortcomings, new electrode materials with a high specific surface area, short ion-transfer path and continuous pore network are still needed to be explored depending on the specific requirements. Moreover, as aforementioned, integrated systems and smart multifunctional energy storage devices are still needed to be developed to fulfill the current requirements. Future research should consider more work to conquer the current drawbacks and expedite the advent of new generations of flexible and wearable electronic devices.

Acknowledgements

This work was supported by the National Natural Science Foundation of China (51272186, 21422105). Q. Yuan thanks the Large-scale Instrument and Equipment Sharing Foundation of Wuhan University.

Notes and references

1 B. Dunn, H. Kamath and J. M. Tarascon, *Science*, 2011, **334**, 928.
2 A. Manthiram, A. V. Murugan, A. Sarkar and T. Muraliganth, *Energy Environ. Sci.*, 2008, **1**, 621.
3 D. J. Lipomi, B. C. K. Tee, M. Vosgueritchian and Z. Bao, *Adv. Mater.*, 2011, **23**, 1771.
4 Y. G. Sun, W. M. Choi, H. Jiang, Y. Y. Huang and J. A. Rogers, *Nat. Nanotechnol.*, 2006, **1**, 201.
5 J. Yoon, A. J. Baca, S. I. Park, P. Elvikis, J. B. Geddes, L. Li 3rd, R. H. Kim, J. Xiao, S. Wang, T. H. Kim, M. J. Motala, B. Y. Ahn, E. B. Duoss, J. A. Lewis, R. G. Nuzzo, P. M. Ferreira, Y. Huang, A. Rockett and J. A. Rogers, *Nat. Mater.*, 2008, **7**, 907.
6 A. M. Gaikwad, A. M. Zamarayeva, J. Rousseau, H. Chu, I. Derin and D. A. Steingart, *Adv. Mater.*, 2012, **24**, 5071.
7 C. Wang, W. Zheng, Z. Yue, C. O. Too and G. G. Wallace, *Adv. Mater.*, 2011, **23**, 3580.
8 D. Kim, G. Shin, Y. J. Kang, W. Kim and J. S. Ha, *ACS Nano*, 2013, **7**, 7975.
9 C. J. Yu, C. Masarapu, J. Rong, B. Wei and H. Jiang, *Adv. Mater.*, 2009, **21**, 4793.
10 L. B. Hu, M. Pasta, F. L. Mantia, L. Cui, S. Jeong, H. D. Deshazer, J. W. Choi, S. M. Han and Y. Cui, *Nano Lett.*, 2010, **10**, 708.
11 X. Li, T. Gu and B. Wei, *Nano Lett.*, 2012, **12**, 6366.
12 B. Yue, C. Wang, X. Ding and G. G. Wallace, *Electrochim. Acta*, 2012, **68**, 18.
13 Z. Q. Niu, H. B. Dong, B. W. Zhu, J. Z. Li, H. H. Hng, W. Y. Zhou, X. D. Chen and S. S. Xie, *Adv. Mater.*, 2013, **25**, 1058.
14 Z. Yang, J. Deng, X. Chen, J. Ren and H. Peng, *Angew. Chem., Int. Ed.*, 2013, **52**, 13453.
15 C. Zhao, C. Wang, Z. Yue, K. Shu and G. G. Wallace, *ACS Appl. Mater. Interfaces*, 2013, **5**, 9008.
16 G. Zhou, F. Li and H. M. Cheng, *Energy Environ. Sci.*, 2014, **7**, 1307.
17 Y. G. Wang and Y. Y. Xia, *Adv. Mater.*, 2013, **25**, 5336.
18 Z. Song, T. Ma, R. Tang, Q. Cheng, X. Wang, D. Krishnaraju, R. Panat, C. K. Chan, H. Yu and H. Jiang, *Nat. Commun.*, 2014, **5**, 3140.
19 X. W. Yang, C. Cheng, Y. F. Wang, L. Qiu and D. Li, *Science*, 2013, **341**, 534.
20 V. L. Pushparaj, M. M. Shaijumon, A. Kumar, S. Murugesan, L. Ci, R. Vajtai, R. J. Linhardt, O. Nalamasu and P. M. Ajayan, *Proc. Natl. Acad. Sci. U. S. A.*, 2007, **104**, 13574.
21 K. Xie and B. Wei, *Adv. Mater.*, 2014, **22**, 3592.
22 Y. Huang, J. Liang and Y. Chen, *Small*, 2012, **8**, 1805.
23 Y. Sun, Q. Wu and G. Shi, *Energy Environ. Sci.*, 2011, **4**, 1113.
24 P. Simon and Y. Gogotsi, *Nat. Mater.*, 2008, **7**, 845.
25 X. Yu, B. Lu and Z. Xu, *Adv. Mater.*, 2014, **26**, 1044.
26 Z. Yu, X. Niu, Z. Liu and Q. Pei, *Adv. Mater.*, 2011, **23**, 3989.
27 G. Shin, M. Y. Bae, H. J. Lee, S. K. Hong, C. H. Yoon, G. Zi, J. A. Rogers and J. S. Ha, *ACS Nano*, 2011, **5**, 10009.
28 S. Cheng and Z. Wu, *Lab Chip*, 2010, **10**, 3227.
29 G. Shin, C. H. Yoon, M. Y. Bae, Y. C. Kim, S. K. Hong, J. A. Rogers and J. S. Ha, *Small*, 2011, **7**, 1181.
30 S. C. Mannsfeld, B. C. Tee, R. M. Stoltenberg, C. V. Chen, S. Barman, B. V. Muir, A. N. Sokolov, C. Reese and Z. Bao, *Nat. Mater.*, 2010, **9**, 859.
31 T. Yamada, Y. Hayamizu, Y. Yamamoto, Y. Yomogida, A. Izadi-Najafabadi, D. N. Futaba and K. Hata, *Nat. Nanotechnol.*, 2011, **6**, 296.
32 C. Yu, Z. Wang, H. Yu and H. Jiang, *Appl. Phys. Lett.*, 2009, **95**, 141912.
33 D. J. Lipomi, M. Vosgueritchian, B. C. Tee, S. L. Hellstrom, J. A. Lee, C. H. Fox and Z. Bao, *Nat. Nanotechnol.*, 2011, **6**, 788.
34 D. Son, J. Lee, S. Qiao, R. Ghaffari, J. Kim, J. E. Lee, C. Song, S. J. Kim, D. J. Lee, S. W. Jun, S. Yang, M. Park, J. Shin, K. Do, M. Lee, K. Kang, C. S. Hwang, N. Lu, T. Hyeon and D.-H. Kim, *Nat. Nanotechnol.*, 2014, **9**, 397.
35 S. Park and S. Jayaraman, *MRS Bull.*, 2003, **28**, 585.
36 G. M. Zhou, F. Li and H. M. Cheng, *Energy Environ. Sci.*, 2014, **7**, 1307.
37 Y. Cheng and J. Liu, *Mater. Res. Lett.*, 2013, **1**, 175.
38 G. Wang, X. Lu, Y. Ling, T. Zhai, H. Wang, Y. Tong and Y. Li, *ACS Nano*, 2012, **6**, 10296.

39 X. Lu, M. Yu, G. Wang, T. Zhai, S. Xie, Y. Ling, Y. Tong and Y. Li, *Adv. Mater.*, 2013, **25**, 267.
40 K. Wang, Q. Meng, Y. Zhang, Z. Wei and M. Miao, *Adv. Mater.*, 2013, **25**, 1494.
41 Y. J. Kang, H. Chun, C.-H. Han and W. Kim, *Nanotechnology*, 2012, **23**, 065401.
42 B. E. Conway, *Electrochemical Supercapacitors, Scientific Fundamentals and Technological Applications*, Kluwer Academic/Plenum, New York, 1999.
43 K. Wang, H. P. Wu, Y. N. Meng and Z. X. Wei, *Small*, 2014, **10**, 14.
44 Z. Zhang, J. Deng, X. Li, Z. Yang, S. He, X. Chen, G. Guan, J. Ren and H. Peng, *Adv. Mater.*, 2015, **27**, 356.
45 L. Kou, T. Huang, B. Zheng, Y. Han, X. Zhao, K. Gopalsamy, H. Sun and C. Gao, *Nat. Commun.*, 2014, 5.
46 Q. Meng, K. Wang, W. Guo, J. Fang, Z. Wei and X. She, *Small*, 2014, **10**, 3187.
47 J. Ren, L. Li, C. Chen, X. Chen, Z. Cai, L. Qiu, Y. Wang, X. Zhu and H. Peng, *Adv. Mater.*, 2013, **25**, 1155.
48 M. F. El-Kady and R. B. Kaner, *Nat. Commun.*, 2013, **4**, 9.
49 L. J. Pan, G. H. Yu, D. Y. Zhai, H. R. Lee, W. T. Zhao, N. Liu, H. L. Wang, B. C. K. Tee, Y. Shi, Y. Cui and Z. N. Bao, *Proc. Natl. Acad. Sci. U. S. A.*, 2012, **109**, 9287.
50 Y. Shi, L. Pan, B. Liu, Y. Wang, Y. Cui, Z. Bao and G. Yu, *J. Mater. Chem. A*, 2014, **2**, 6086.
51 B. D. Gate, *Science*, 2009, **323**, 1566.
52 L. Nyholm, G. Nystrom, A. Mihranyan and M. Stromme, *Adv. Mater.*, 2011, **23**, 3751.
53 N. S. Liu, W. Z. Ma, J. Y. Tao, X. H. Zhang, J. Su, L. Y. Li, C. X. Yang, Y. H. Gao, D. Golberg and Y. Bando, *Adv. Mater.*, 2013, **25**, 4925.
54 J. Ren, W. Y. Bai, G. Z. Guan, Y. Zhang and H. S. Peng, *Adv. Mater.*, 2013, **25**, 5965.
55 Y. W. Cheng, S. T. Lu, H. B. Zhang, C. V. Varanasi and J. Liu, *Nano Lett.*, 2012, **12**, 4206.
56 M. Kaempgen, C. K. Chan, J. Ma, Y. Cui and G. Gruner, *Nano Lett.*, 2009, **9**, 1872.
57 G. H. Yu, L. B. Hu, N. A. Liu, H. L. Wang, M. Vosgueritchian, Y. Yang, Y. Cui and Z. A. Bao, *Nano Lett.*, 2011, **11**, 4438.
58 Z. Q. Niu, L. L. Liu, L. Zhang, Q. Shao, W. Y. Zhou, X. D. Chen and S. S. Xie, *Adv. Mater.*, 2014, **26**, 3681.
59 G. H. Yu, L. B. Hu, M. Vosgueritchian, H. L. Wang, X. Xie, J. R. McDonough, X. Cui, Y. Cui and Z. N. Bao, *Nano Lett.*, 2011, **11**, 2905.
60 L. L. Zhang, X. Zhao, M. D. Stoller, Y. W. Zhu, H. X. Ji, S. Murali, Y. P. Wu, S. Perales, B. Clevenger and R. S. Ruoff, *Nano Lett.*, 2012, **12**, 1806.
61 Y. Meng, Y. Zhao, C. Hu, H. Cheng, Y. Hu, Z. Zhang, G. Shi and L. Qu, *Adv. Mater.*, 2013, **25**, 2326.
62 F. Meng and Y. Ding, *Adv. Mater.*, 2011, **23**, 4098.
63 Z. Bo, W. Zhu, W. Ma, Z. Wen, X. Shuai, J. Chen, J. Yan, Z. Wang, K. Cen and X. Feng, *Adv. Mater.*, 2013, **25**, 5799.
64 Z. Dong, C. Jiang, H. Cheng, Y. Zhao, G. Shi, L. Jiang and L. Qu, *Adv. Mater.*, 2012, **24**, 1856.
65 L. F. Chen, Z. H. Huang, H. W. Liang, Q. F. Guan and S. H. Yu, *Adv. Mater.*, 2013, **25**, 4746.
66 L. Liu, Z. Niu, L. Zhang and X. Chen, *Small*, 2014, **10**, 2200.
67 S. Y. Yin, Z. Q. Niu and X. D. Chen, *Small*, 2012, **8**, 2458.
68 C. Choi, J. A. Lee, A. Y. Choi, Y. T. Kim, X. Lepró, M. D. Lima, R. H. Baughman and S. J. Kim, *Adv. Mater.*, 2014, **26**, 2059.
69 Q. Meng, H. Wu, Y. Meng, K. Xie, Z. Wei and Z. Guo, *Adv. Mater.*, 2014, **26**, 4100.
70 S. Wagner and S. Bauer, *MRS Bull.*, 2012, **37**, 207.
71 L. Xiao, Z. Chen, C. Feng, L. Liu, Z. Q. Bai, Y. Wang, L. Qian, Y. Y. Zhang, Q. Q. Li, K. L. Jiang and S. S. Fan, *Nano Lett.*, 2008, **8**, 4539.
72 K. S. Kim, Y. Zhao, H. Jang, S. Y. Lee, J. M. Kim, J. H. Ahn, P. Kim, J. Y. Choi and B. H. Hong, *Nature*, 2009, **457**, 706.
73 D. Y. Khang, H. Q. Jiang, Y. Huang and J. A. Rogers, *Science*, 2006, **311**, 208.
74 D. H. Kim, J. H. Ahn, W. M. Choi, H. S. Kim, T. H. Kim, J. Z. Song, Y. G. Y. Huang, Z. J. Liu, C. Lu and J. A. Rogers, *Science*, 2008, **320**, 507.
75 T. Sekitani, Y. Noguchi, K. Hata, T. Fukushima, T. Aida and T. Someya, *Science*, 2008, **321**, 1468.
76 M. Ramuz, B. C. K. Tee, J. B. H. Tok and Z. N. Bao, *Adv. Mater.*, 2012, **24**, 3223.
77 Y. Zhu and F. Xu, *Adv. Mater.*, 2012, **24**, 1073.
78 P. Lee, J. Lee, H. Lee, J. Yeo, S. Hong, K. H. Nam, D. Lee, S. S. Lee and S. H. Ko, *Adv. Mater.*, 2012, **24**, 3326.
79 H. L. Filiatrault, G. C. Porteous, R. S. Carmichael, G. J. E. Davidson and T. B. Carmichael, *Adv. Mater.*, 2012, **24**, 2673.
80 L. B. Hu, J. W. Choi, Y. Yang, S. Jeong, F. La Mantia, L. F. Cui and Y. Cui, *Proc. Natl. Acad. Sci. U. S. A.*, 2009, **106**, 21490.
81 K. Wang, P. Zhao, X. M. Zhou, H. P. Wu and Z. X. Wei, *J. Mater. Chem.*, 2011, **21**, 16373.
82 W. Chen, R. B. Rakhi, L. Hu, X. Xie, Y. Cui and H. N. Alshareef, *Nano Lett.*, 2011, **11**, 5165.
83 G. Wang, H. Wang, X. Lu, Y. Ling, M. Yu, T. Zhai, Y. Tong and Y. Li, *Adv. Mater.*, 2014, **26**, 2676.
84 J. F. Zang, C. Y. Cao, Y. Y. Feng, J. Liu and X. H. Zhao, *Sci. Rep.*, 2014, **4**, 6492.
85 M.-Q. Zhao, C. E. Ren, Z. Ling, M. R. Lukatskaya, C. Zhang, K. L. Van Aken, M. W. Barsoum and Y. Gogotsi, *Adv. Mater.*, 2015, **27**, 339.
86 C. Z. Meng, C. H. Liu, L. Z. Chen, C. H. Hu and S. S. Fan, *Nano Lett.*, 2010, **10**, 4025.
87 L. Huang, D. Chen, Y. Ding, S. Feng, Z. L. Wang and M. Liu, *Nano Lett.*, 2013, **13**, 3135.
88 Y. Xu, Z. Lin, X. Huang, Y. Wang, Y. Huang and X. Duan, *Adv. Mater.*, 2013, **25**, 5779.
89 K. Jost, C. R. Perez, J. K. McDonough, V. Presser, M. Heon, G. Dion and Y. Gogotsi, *Energy Environ. Sci.*, 2011, **4**, 5060.
90 L. B. Hu, W. Chen, X. Xie, N. A. Liu, Y. Yang, H. Wu, Y. Yao, M. Pasta, H. N. Alshareef and Y. Cui, *ACS Nano*, 2011, **5**, 8904.
91 H. Wang, B. W. Zhu, W. C. Jiang, Y. Yang, W. R. Leow, H. Wang and X. D. Chen, *Adv. Mater.*, 2014, **26**, 3638.
92 L. Y. Yuan, X. Xiao, T. P. Ding, J. W. Zhong, X. H. Zhang, Y. Shen, B. Hu, Y. H. Huang, J. Zhou and Z. L. Wang, *Angew. Chem., Int. Ed.*, 2012, **51**, 4934.

93 Z. Q. Niu, W. Y. Zhou, J. Chen, G. X. Feng, H. Li, Y. S. Hu, W. J. Ma, H. B. Dong, J. Z. Li and S. S. Xie, *Small*, 2013, **9**, 518.
94 H. Zhang, G. Cao, Z. Wang, Y. Yang, Z. Shi and Z. Gu, *Nano Lett.*, 2008, **8**, 2664.
95 C. Niu, E. K. Sichel, R. Hoch, D. Moy and H. Tennent, *Appl. Phys. Lett.*, 1997, **70**, 1480.
96 D. N. Futaba, K. Hata, T. Yamada, T. Hiraoka, Y. Hayamizu, Y. Kakudate, O. Tanaike, H. Hatori, M. Yumura and S. Iijima, *Nat. Mater.*, 2006, **5**, 987.
97 E. Frackowiak, K. Jurewicz, S. Delpeux and F. Beguin, *J. Power Sources*, 2001, **97–98**, 822.
98 T. Bordjiba and L. H. D. M. Mohamedi, *Adv. Mater.*, 2008, **20**, 815.
99 Y. J. Kang, H. Chung, C. H. Han and W. Kim, *Nanotechnology*, 2012, **23**, 065401.
100 Z. Cao and B. B. Wei, *Energy Environ. Sci.*, 2013, **6**, 3183.
101 Z. Zhang, T. Zhai, X. Lu, M. Yu, Y. Tong and K. Mai, *J. Mater. Chem. A*, 2013, **1**, 505.
102 Y.-K. Hsu, Y.-C. Chen, Y.-G. Lin, L.-C. Chen and K.-H. Chen, *J. Mater. Chem.*, 2012, **22**, 3383.
103 V. T. Le, H. Kim, A. Ghosh, J. Kim, J. Chang, Q. A. Vu, D. T. Pham, J.-H. Lee, S.-W. Kim and Y. H. Lee, *ACS Nano*, 2013, **7**, 5940.
104 L. L. Zhang and X. S. Zhao, *Chem. Soc. Rev.*, 2009, **38**, 2520.
105 E. Raymundo-Pinero, M. Cadek, M. Wachtler and F. Beguin, *ChemSusChem*, 2011, **4**, 943.
106 Y. C. Chen, Y. K. Hsu, Y. G. Lin, Y. K. Lin, Y. Y. Horng, L. C. Chen and K. H. Chen, *Electrochim. Acta*, 2011, **56**, 7124.
107 C. K. Chan, H. L. Peng, G. Liu, K. McIlwrath, X. F. Zhang, R. A. Huggins and Y. Cui, *Nat. Nanotechnol.*, 2008, **3**, 31.
108 C. Q. Bian, A. H. Yu and H. Q. Wu, *Electrochem. Commun.*, 2009, **11**, 266.
109 L. Huang, N. Yi, Y. Wu, Y. Zhang, Q. Zhang, Y. Huang, Y. Ma and Y. Chen, *Adv. Mater.*, 2013, **25**, 2224.
110 M. D. Hager, P. Greil, C. Leyens, S. van der Zwaag and U. S. Schubert, *Adv. Mater.*, 2010, **22**, 5424.
111 T. Kakuta, Y. Takashima, M. Nakahata, M. Otsubo, H. Yamaguchi and A. Harada, *Adv. Mater.*, 2013, **25**, 2849.
112 T. S. Wong, S. H. Kang, S. K. Y. Tang, E. J. Smythe, B. D. Hatton, A. Grinthal and J. Aizenberg, *Nature*, 2011, **477**, 443.
113 H. X. Wang, Y. H. Xue, J. Ding, L. F. Feng, X. G. Wang and T. Lin, *Angew. Chem., Int. Ed.*, 2011, **50**, 11433.
114 H. H. Jin, C. L. Mangun, D. S. Stradley, J. S. Moore, N. R. Sottos and S. R. White, *Polymer*, 2012, **53**, 581.
115 Y. Amamoto, J. Kamada, H. Otsuka, A. Takahara and K. Matyjaszewski, *Angew. Chem., Int. Ed.*, 2011, **50**, 1660.
116 B. J. Blaiszik, S. L. B. Kramer, S. C. Olugebefola, J. S. Moore, N. R. Sottos and S. R. White, *Annu. Rev. Mater. Res.*, 2010, **40**, 179.
117 B. J. Blaiszik, S. L. B. Kramer, M. E. Grady, D. A. McIlroy, J. S. Moore, N. R. Sottos and S. R. White, *Adv. Mater.*, 2012, **24**, 398.
118 D. Habault, H. Zhang and Y. Zhao, *Chem. Soc. Rev.*, 2013, **42**, 7244.
119 H. Kuroki, I. Tokarev, D. Nykypanchuk, E. Zhulina and S. Minko, *Adv. Funct. Mater.*, 2013, **23**, 4593.
120 Y. Li, L. Li and J. Q. Sun, *Angew. Chem., Int. Ed.*, 2010, **49**, 6129.
121 X. L. Wang, X. J. Liu, F. Zhou and W. M. Liu, *Chem. Commun.*, 2011, **47**, 2324.
122 X. Wang, F. Liu, X. W. Zheng and J. Q. Sun, *Angew. Chem., Int. Ed.*, 2011, **50**, 11378.
123 H. P. Cong, P. Wang and S. H. Yu, *Chem. Mater.*, 2013, **25**, 3357.
124 M. M. Zhang, D. H. Xu, X. Z. Yan, J. Z. Chen, S. Y. Dong, B. Zheng and F. H. Huang, *Angew. Chem., Int. Ed.*, 2012, **51**, 7011.
125 C. Wang, N. Liu, R. Allen, J. B.-H. Tok, Y. P. Wu, F. Zhang, Y. S. Chen and Z. N. Bao, *Adv. Mater.*, 2013, **25**, 5785.
126 A. K. Geim and K. S. Novoselov, *Nat. Mater.*, 2007, **6**, 183.
127 C. N. R. Rao, A. K. Sood, K. S. Subrahmanyam and A. Govindaraj, *Angew. Chem., Int. Ed.*, 2009, **48**, 7752.
128 M. J. Allen, V. C. Tung and R. B. Kaner, *Chem. Rev.*, 2010, **110**, 132.
129 M. Pumera, *Chem. Soc. Rev.*, 2010, **39**, 4146.
130 Y. W. Zhu, S. Murali, W. W. Cai, X. S. Li, J. W. Suk, J. R. Potts and R. S. Ruoff, *Adv. Mater.*, 2010, **22**, 3906.
131 M. D. Stoller, S. Park, Y. Zhu, J. An and R. S. Ruoff, *Nano Lett.*, 2008, **8**, 3498.
132 Z. Q. Niu, L. Zhang, L. L. Liu, B. W. Zhu, H. B. Dong and X. D. Chen, *Adv. Mater.*, 2013, **25**, 4035.
133 Y. Meng, K. Wang, Y. J. Zhang and Z. X. Wei, *Adv. Mater.*, 2013, **25**, 6985.
134 X. Cao, Y. Shi, W. Shi, G. Lu, X. Huang, Q. Yuan, Q. Zhang and H. Zhang, *Small*, 2011, **7**, 3163.
135 F. Liu, S. Song, D. Xue and H. Zhang, *Adv. Mater.*, 2012, **24**, 1089.
136 X. Yang, J. Zhu, L. Qiu and D. Li, *Adv. Mater.*, 2011, **23**, 2833.
137 Y. Xu, K. Sheng, C. Li and G. Shi, *ACS Nano*, 2010, **4**, 4324.
138 C. Li and G. Shi, *Nanoscale*, 2012, **4**, 5549.
139 Y. N. Meng, Y. Zhao, C. G. Hu, H. H. Cheng, Y. Hu, Z. P. Zhang, G. Q. Shi and L. T. Qu, *Adv. Mater.*, 2013, **25**, 2326.
140 C. Z. Yuan, B. Gao, L. F. Shen, S. D. Yang, L. Hao, X. J. Lu, F. Zhang, L. J. Zhang and X. G. Zhang, *Nanoscale*, 2011, **3**, 529.
141 C. Liu, F. Li, L. P. Ma and H. M. Cheng, *Adv. Mater.*, 2010, **22**, E28.
142 Z. B. Lei, N. Christov and X. S. Zhao, *Energy Environ. Sci.*, 2011, **4**, 1866.
143 Z. Chen, Y. C. Qin, D. Weng, Q. F. Xiao, Y. T. Peng, X. L. Wang, H. X. Li, F. Wei and Y. F. Lu, *Adv. Funct. Mater.*, 2009, **19**, 3420.
144 Y. Yang, H. L. Fei, G. D. Ruan, C. S. Xiang and J. M. Tour, *Adv. Mater.*, 2014, **26**, 8163.
145 M. Yu, T. Zhai, X. Lu, X. Chen, S. Xie, W. Li, C. Liang, W. Zhao, L. Zhang and Y. Tong, *J. Power Sources*, 2013, **239**, 64.
146 X. H. Lu, T. Zhai, X. H. Zhang, Y. Q. Shen, L. Y. Yuan, B. Hu, L. Gong, J. Chen, Y. H. Gao, J. Zhou, Y. X. Tong and Z. L. Wang, *Adv. Mater.*, 2012, **24**, 938.

147 G. A. Snook, P. Kao and A. S. Best, *J. Power Sources*, 2011, **196**, 1.
148 K. Naoi and M. Morita, *Electrochem. Soc. Interface*, 2008, **17**, 44.
149 Q. Zhang, E. Uchaker, S. L. Candelaria and G. Cao, *Chem. Soc. Rev.*, 2013, **42**, 3127.
150 L. L. Zhang and X. S. Zhao, *Chem. Soc. Rev.*, 2009, **38**, 2520.
151 S. L. Candelaria, Y. Shao, W. Zhou, X. Li, J. Xiao, J.-G. Zhang, Y. Wang, J. Liu, J. Li and G. Cao, *Nano Energy*, 2012, **1**, 195.
152 G. Wang, L. Zhang and J. Zhang, *Chem. Soc. Rev.*, 2012, **41**, 797.
153 S. Liu, S. Sun and X.-Z. You, *Nanoscale*, 2014, **6**, 2037.
154 X. Sun, T. Chen, S. Huang, L. Li and H. Peng, *Chem. Soc. Rev.*, 2010, **39**, 4244.
155 H. Wei, X. Yan, S. Wu, Z. Luo, S. Wei and Z. Guo, *J. Phys. Chem. C*, 2012, **116**, 25052.
156 X. L. Chen, H. J. Lin, P. N. Chen, G. Z. Guan, J. Deng and H. S. Peng, *Adv. Mater.*, 2014, **26**, 4444.
157 L. Nyholm, G. Nyström, A. Mihranyan and M. Strømme, *Adv. Mater.*, 2013, **23**, 3751.
158 M. Mastragostino, C. Arbizzani and F. Soavi, *J. Power Sources*, 2001, **97–98**, 812.
159 Y. Cheng, S. Lu, H. Zhang, C. V. Varanasi and J. Liu, *Nano Lett.*, 2012, **12**, 4206.
160 Y. Zhu, S. Murali, M. D. Stoller, K. J. Ganesh, W. Cai, P. J. Ferreira, A. Pirkle, R. M. Wallace, K. A. Cychosz, M. Thommes, D. Su, E. A. Stach and R. S. Ruoff, *Science*, 2011, **332**, 1537.
161 C. Choi, J. A. Lee, A. Y. Choi, Y. T. Kim, X. Lepró, M. D. Lima, R. H. Baughman and S. J. Kim, *Adv. Mater.*, 2014, **26**, 2059.
162 X. H. Cao, B. Zheng, W. H. Shi, J. Yang, Z. X. Fan, Z. M. Luo, X. H. Rui, B. Chen, Q. Y. Yan and H. Zhang, *Adv. Mater.*, 2015, **27**, 4695.
163 X. F. Wang, X. H. Lu, B. Liu, D. Chen, Y. X. Tong and G. Z. Shen, *Adv. Mater.*, 2014, **26**, 4763.
164 X. Xiao, X. Peng, H. Y. Jin, T. Q. Li, C. C. Zhang, B. Gao, B. Hu, K. F. Huo and J. Zhou, *Adv. Mater.*, 2013, **25**, 5091.
165 M. H. Yu, Y. F. Zhang, Y. X. Zeng, M.-S. Balogun, K. C. Mai, Z. S. Zhang, X. H. Lu and Y. X. Tong, *Adv. Mater.*, 2014, **26**, 4724.
166 L. L. Liu, Z. Q. Niu, L. Zhang, W. Y. Zhou, X. D. Chen and S. S. Xie, *Adv. Mater.*, 2014, **26**, 4855.
167 S. Gao, Y. H. Sun, F. C. Lei, L. Liang, J. W. Liu, W. T. Bi, B. C. Pan and Y. Xie, *Angew. Chem., Int. Ed.*, 2014, **53**, 12789.
168 L.-F. Chen, Z.-H. Huang, H.-W. Liang, Q.-F. Guan and S.-H. Yu, *Adv. Mater.*, 2013, **25**, 4746.
169 C. Z. Yuan, L. Yang, L. R. Hou, L. F. Shen, X. G. Zhang and X. W. Lou, *Energy Environ. Sci.*, 2012, **5**, 7883.
170 C. Z. Yuan, X. G. Zhang, L. R. Hou, L. F. Shen, D. K. Li, F. Zhang, C. G. Fan and J. M. Li, *J. Mater. Chem.*, 2010, **20**, 10809.
171 X. Huang, C. Tan, Z. Yin and H. Zhang, *Adv. Mater.*, 2014, **26**, 2185.
172 X. Huang, Z. Y. Zeng and H. Zhang, *Chem. Soc. Rev.*, 2013, **42**, 1934.
173 L. J. Cao, S. B. Yang, W. Gao, Z. Liu, Y. J. Gong, L. L. Ma, G. Shi, S. D. Lei, Y. H. Zhang, S. T. Zhang, R. Vajtai and P. M. Ajayan, *Small*, 2013, **9**, 2905.
174 G. Z. Sun, X. Zhang, R. Z. Lin, J. Yang, H. Zhang and P. Chen, *Angew. Chem., Int. Ed.*, 2015, **54**, 4651.
175 Z. Q. Niu, W. Y. Zhou, X. D. Chen, J. Chen and S. S. Xie, *Adv. Mater.*, 2015, **27**, 6002.
176 F. H. Meng and Y. Ding, *Adv. Mater.*, 2011, **23**, 4098.
177 J. Chmiola, C. Largeot, P. L. Taberna, P. Simon and Y. Gogotsi, *Science*, 2010, **328**, 480.
178 D. Pech, M. Brunet, H. Durou, P. H. Huang, V. Mochalin, Y. Gogotsi, P. L. Taberna and P. Simon, *Nat. Nanotechnol.*, 2010, **5**, 651.
179 X. Y. Lang, A. Hirata, T. Fujita and M. W. Chen, *Nat. Nanotechnol.*, 2011, **6**, 232.
180 J. Y. Yoo, K. Balakrishnan, J. S. Huang, V. Meunier, B. G. Sumpter, A. Srivastava, M. Conway, A. L. M. Reddy, J. Yu, R. Vajtai and P. M. Ajayan, *Nano Lett.*, 2011, **11**, 1423.
181 J. Feng, X. Sun, C. Z. Wu, L. L. Peng, C. W. Lin, S. L. Hu, J. L. Yang and Y. Xie, *J. Am. Chem. Soc.*, 2011, **133**, 17832.
182 Y. M. He, W. J. Chen, J. Yuan Zhou, X. D. Li, P. Y. Tang, Z. X. Zhang, J. C. Fu and E. Q. Xie, *ACS Appl. Mater. Interfaces*, 2014, **6**, 210.
183 C. W. Shen, X. H. Wang, W. F. Zhang and F. Y. Kang, *J. Power Sources*, 2011, **196**, 10465.
184 W. Sun and X. Y. Chen, *J. Power Sources*, 2009, **193**, 924.
185 M. Q. Xue, F. W. Li, J. Zhu, H. Song, M. N. Zhang and T. B. Cao, *Adv. Funct. Mater.*, 2012, **22**, 1284.
186 K. Wang, W. J. Zou, B. G. Quan, A. F. Yu, H. P. Wu, P. Jiang and Z. X. Wei, *Adv. Energy Mater.*, 2011, **1**, 1068.
187 M. F. El-Kady and R. B. Kaner, *Nat. Commun.*, 2013, **4**, 1475.
188 Q. H. Meng, H. P. Wu, Y. N. Meng, K. Xie, Z. X. Wei and Z. X. Guo, *Adv. Mater.*, 2014, **26**, 4100.
189 H. Sun, X. You, J. Deng, X. L. Chen, Z. B. Yang, J. Ren and H. S. Peng, *Adv. Mater.*, 2014, **26**, 2868.
190 Z. S. Wu, A. Winter, L. Chen, Y. Sun, A. Turchanin, X. L. Feng and K. Mullen, *Adv. Mater.*, 2012, **24**, 5130.
191 B. Liu, B. Y. Liu, X. F. Wang, X. H. Wu, W. N. Zhao, Z. M. Xu, D. Chen and G. Z. Shen, *Adv. Mater.*, 2014, **26**, 4999.
192 N. A. Choudhury, S. Sampath and A. K. Shukla, *Energy Environ. Sci.*, 2009, **2**, 55.
193 L. Yuan, X.-H. Lu, X. Xiao, T. Zhai, J. Dai, F. Zhang, B. Hu, X. Wang, L. Gong, J. Chen, C. Hu, Y. Tong, J. Zhou and Z. L. Wang, *ACS Nano*, 2012, **6**, 656.
194 K. Wang, X. Zhang, C. Li, X. Z. Sun, Q. H. Meng, Y. W. Ma and Z. X. Wei, *Adv. Mater.*, 2015, **27**, 7451.
195 R. Chen, F. Wu, L. Li, B. Xu, X. Qiu and S. Chen, *J. Phys. Chem. C*, 2007, **111**, 5184.
196 A. Balducci, R. Dugas, P. L. Taberna, P. Simon, D. Plee, M. Mastragostino and S. Passerini, *J. Power Sources*, 2007, **165**, 922.
197 X. H. Liu, D. B. Wu, H. L. Wang and Q. G. Wang, *Adv. Mater.*, 2014, **26**, 4370.
198 X. F. Wang, B. Liu, Q. F. Wang, W. F. Song, X. J. Hou, D. Chen, Y. B. Cheng and G. Z. Shen, *Adv. Mater.*, 2013, **25**, 1479.

199 X. H. Xia, J. S. Luo, Z. Y. Zeng, C. Guan, Y. Q. Zhang, J. P. Tu, H. Zhang and H. J. Fan, *Sci. Rep.*, 2012, **2**, 981.
200 Q. Yang, Y. Liu, Z. Li, Z. Yang, X. Wang and Z. L. Wang, *Angew. Chem.*, 2012, **124**, 6549.
201 X. F. Wang, B. Liu, R. Liu, Q. F. Wang, X. J. Hou, D. Chen, R. M. Wang and G. Z. Shen, *Angew. Chem., Int. Ed.*, 2014, **53**, 1849.
202 T. N. Murakami, N. Kawashima and T. Miyasaka, *Chem. Commun.*, 2005, 3346.
203 Z. Yang, L. Li, Y. Luo, R. He, L. Qiu, H. Lin and H. Peng, *J. Mater. Chem.*, 2013, **1**, 954.
204 W. Guo, X. Xue, S. Wang, C. Lin and Z. L. Wang, *Nano Lett.*, 2012, **12**, 2520.
205 G. Wee, T. Salim, Y. M. Lam, S. G. Mhaisalkar and M. Srinivasan, *Energy Environ. Sci.*, 2011, **4**, 413.
206 N. S. Lewis, *Science*, 2007, **315**, 798.
207 Y. Zhang, Y. Zhao, X. L. Cheng, W. Weng, J. Ren, X. Fang, Y. S. Jiang, P. N. Chen, Z. T. Zhang, Y. G. Wang and H. S. Peng, *Angew. Chem., Int. Ed.*, 2015, **54**, 11177.
208 Z. T. Zhang, X. L. Chen, P. N. Chen, G. Z. Guan, L. B. Qiu, H. J. Lin, Z. B. Yang, W. Y. Bai, Y. F. Luo and H. S. Peng, *Adv. Mater.*, 2014, **26**, 466.